Super-resolution in Imaging High Contrast Targets from the Perspective of Scattering Coefficients

Habib Ammari[☆]

Department of Mathematics, ETH Zürich, Rämistrasse 101, CH-8092 Zürich, Switzerland.

Yat Tin Chow[,☆☆]

Department of Mathematics, University of California, Los Angeles, CA 90095-1555, USA.

Jun Zou [*]

Department of Mathematics, Chinese University of Hong Kong, Shatin, N.T., Hong Kong.

Abstract

In this paper we consider the inverse scattering problem for high-contrast targets, and analyze mathematically the experimentally observed phenomenon about super-resolution in imaging the shapes of these targets. In particular, super-resolution at specific high contrast values is justified based on the novel concept of scattering coefficients and several important implications (given by two main theorems, Theorems 4.6 and 4.9). This is the first time that a mathematical theory of super-resolution is established in the context of imaging high-contrast inclusions. We shall also illustrate our main findings with a variety of numerical examples. These findings may help develop resonant structures for resolution enhancement.

Keywords: inverse scattering, super-resolution, scattering coefficients
2010 MSC: 35B30, 35R30

1. Introduction

The aim of this work is to mathematically investigate the mechanism underlying the experimentally-observed phenomenon of super-resolution in reconstructing targets of high contrast from far-field measurements. Our main focus is to explore the possibility of breaking the diffraction barrier from the far-field measurements using the novel concept of scattering coefficients [1, 2, 3]. This diffraction barrier, referred to as the Abbe-Rayleigh or the resolution limit, places a fundamental limit on the minimal distance at which we can resolve the shape of a target [4, 5]. It applies only to waves that have propagated for a distance substantially larger than its wavelength [6, 7].

Since the mid-20th century, several approaches have aimed at pushing this diffraction limits. Resolution enhancement in imaging the target shape from far-field measurements can be achieved using sub-wavelength-scaled resonant media [8, 9, 10, 11, 12, 13], single molecule imaging [14] and using plasmonic particles [15]. Another innovative method to overcome the diffraction barrier has been proposed after some experimental observations in [16]. In their work, resolution enhancement in shape reconstruction of the inclusion was experimentally shown when the contrast value is very high. In the reconstructed images

[☆]The work of this author was supported by the ERC Advanced Grant Project MULTIMOD–267184.
[☆☆]The work of this author was supported by NSF Grant ECCS-1462398.
[*]Corresponding author. The work of this author was substantially supported by Hong Kong RGC grants (projects 14306814 and 405513).

Email addresses: habib.ammari@math.ethz.ch (Habib Ammari[☆]), ytchow@math.cuhk.edu.hk (Yat Tin Chow[,☆☆]), zou@math.cuhk.edu.hk (Jun Zou)

from far-field measurements, the observed resolution is smaller than half of the operating wavelength. This encouraging observation suggests a possibility of breaking the resolution limit with high permittivity of the target. It is therefore the purpose of this work to prove that the higher the permittivity of the target is, the higher the resolving power is in imaging its shape.

For the transmission problem of a strictly convex domain, it was proved in [17] that there exists an infinite sequence of complex resonant frequencies located at the upper half plane. These resonances converge to the real axis exponentially fast, and the real part of these resonances correspond to the quasi-resonant modes introduced as in [17]. Quasi-resonance occurs when the wavelength inside the inclusion is larger than the wavelength in the background media and is such that it reaches the real part of one of these true resonant frequencies. In this paper, we have shown, via the analysis of the shape derivative of the scattering coefficients, that these resonant state of the inclusion actually has a signature in the far-field and can be used for super-resolved imaging from far-field data. To be more exact, we have proved that, in the shape derivative of the scattering coefficients for a circular domain, there are simple poles at the complex resonant states, and therefore peaks corresponding to the real parts of these resonances. Henceforth, as the material contrast increases to infinity and is such that it is equal to the real part of a resonance, the sensitivity in the scattering coefficients becomes large and super-resolution for imaging becomes possible.

Throughout this paper, we consider the following scattering problem in $\mathbb{R}^2$,

$$\Big(\Delta + k^2\Big(1 + q(x)\Big)\Big)u = 0, \tag{1.1}$$

where u is the total field, $q(x) > 0$ is the contrast of the medium and k is the wave number. The operating wavelength is then $2\pi/k$.

We consider an inclusion D contained inside a homogeneous background medium, and assume that D is an open bounded connected domain with a $\mathcal{C}^{1,\alpha}$-boundary for some $\alpha > 0$. Suppose that the function q is of the form

$$q(x) = \varepsilon^* \chi_D(x), \tag{1.2}$$

where χ_D denotes the characteristic function of D and $\varepsilon^* > 0$ is a constant. We shall always complement the system (1.1) by the physical outgoing Sommerfeld radiation condition:

$$\Big|\frac{\partial}{\partial|x|}u^s - iku^s\Big| = O(|x|^{-\frac{3}{2}}) \quad \text{as} \quad |x| \to \infty\,, \tag{1.3}$$

where $u^s := u - u^i$ is the scattered field and u^i is the incident field. The solution u to the system (1.1)-(1.3) represents the total field due to the scattering from the inclusion D corresponding to the incident field u^i.

Following the work of [18, 2, 3], the scattering coefficients provide a powerful and efficient tool for shape classification of the target D. Therefore, we aim at exhibiting the mechanism underlying the super-resolution phenomenon experimentally-observed in [16] in terms of the scattering coefficients corresponding to high-contrast inclusions.

In [2], it is proved that the scattering coefficient of order (n, m) decays very quickly as the orders $|n|$, $|m|$ increase. Nonetheless, it is shown in [3] that the scattering coefficients can be stably reconstructed from the far-field measurements by a least-squares method. The stability of the reconstruction in the presence of a measurement noise is analyzed and the resolving power of the reconstruction in terms of the signal-to-noise-ratio is estimated. It is the purpose of this paper to use the scattering coefficients to estimate the resolution limit for imaging high contrast targets from far-field measurements as function of the material contrast, and to prove that the higher the permittivity is inside the target, the better the resolution is for imaging its shape from far-field measurements.

In order to achieve this goal, in this work, we first give a decay estimate of the scattering coefficients in arbitrary shaped domains, and then in the particular case of a circular domain. Our estimate shows different behaviors of the scattering coefficients of different orders as the material contrast increases. Then we provide a sensitivity analysis of the scattering coefficients, which clearly shows that, in the

linearized case, the scattering coefficient of order (n, m) of a circular domain contains information about the $(n-m)$-th Fourier mode of the shape perturbation. Afterwards, we establish the asymptotic behavior of eigenvalues of an important family of integral operators closely related to the scattering coefficients. Series representations of the scattering coefficients and their shape derivatives in the case of a circular domain are given based on this asymptotic behavior. From these series representations, we prove that as the material contrast increases and moves close to the reciprocal of the eigenvalues, the shape derivatives of the scattering coefficients behave like simple poles. This explains the better conditioning of the inversion process of higher Fourier modes of inclusions with large material contrast, and hence an enhanced resolution of reconstructing the perturbation using the scattering coefficients. Numerical examples illustrate that the relative magnitudes of higher order scattering coefficients grow as the medium coefficients grow and move close to the reciprocals of several of these eigenvalues similtaneously, therefore providing more information about the shape of the domain with a fixed signal-to-noise ratio. Our approach provides a good and promising direction of understanding towards the super-resolution phenomenon for high-contrast targets.

This paper is organized as follows. In section 2 we give a brief review of the concept of scattering coefficients. We also prove a fundamental expression of the scattering coefficients in terms of a family of important integral operators. Sensitivity analysis of the scattering coefficients with a fixed contrast is then presented in section 3, which shows that the shape derivative can also be represented by the family of integral operators introduced in section 2. Section 4.1 briefly recalls Riesz decomposition of compact operators. Asymptotic behavior of eigenvalues and eigenfunctions of the introduced integral operators will be studied in section 4.2. Section 4.3 provides a series representation of the scattering coefficients and their shape derivative. A mathematical explanation of the super-resolution phenomenon is given based on several implications in Theorems 4.6 and 4.9, which are the main results of this work. Theorem 4.6 provides the clear asymptotic behavior of the eigenvalues of a related operator, while Theorem 4.9 gives a reason for the stronger sensitivity of the Fourier modes of higher orders when the reciprocal of a contrast comes close to the real parts of the reciprocals of the respective eigenvalues simultaneously. Numerical results are reported in section 5 to illustrate the phenomenon of super-resolution as the material contrast increases.

2. The concept of scattering coefficients and a fundamental expression

In this section, we estimate the behavior of the scattering coefficients. Without loss of generality, from now on, we normalize the wave number k in (1.1) to be $k = 1$ by a change of variables.

To begin with, we first recall the definition of the scattering coefficients $W_{nm}(D, \varepsilon^*)$ from [18, 2]. For this purpose, we introduce the following several notions. The fundamental solution Φ to the Helmholtz operator $\Delta + 1$ in two dimensions satisfying

$$(\Delta + 1)\Phi(x) = \delta_0(x), \tag{2.1}$$

where δ_0 is the Dirac mass at 0, with the outgoing Sommerfeld radiation condition:

$$\big|\frac{\partial}{\partial|x|}\Phi - i\Phi\big| = O(|x|^{-\frac{3}{2}}) \quad \text{as} \quad |x| \to \infty\,,$$

is given by

$$\Phi(x) = -\frac{i}{4}H_0^{(1)}(|x|)\,, \tag{2.2}$$

where $H_0^{(1)}$ is the Hankel function of the first kind of order zero.

Now, given an incident field u^i satisfying the homogeneous Helmholtz equation, i.e.,

$$\Delta u^i + u^i = 0\,, \tag{2.3}$$

the solution u to (1.1) and (1.3) can be readily represented by the Lippmann-Schwinger equation as

$$u(x) = u^i(x) - \varepsilon^* \int_D \Phi(x-y)u(y)dy\,, \quad x \in \mathbb{R}^2\,, \tag{2.4}$$

and hence, the scattered field reads

$$u^s(x) = -\varepsilon^* \int_D \Phi(x-y)u(y)dy\,, \quad x \in \mathbb{R}^2\,. \tag{2.5}$$

Let $S_{\partial D}$ be the single-layer potential defined by the kernel $\Phi(\,\cdot\,)$, i.e.,

$$S_{\partial D}[\phi](x) = \int_{\partial D} \Phi(x-y)\phi(y)\,ds(y) \tag{2.6}$$

for $\phi \in L^2(\partial D)$. Let $S_{\partial D}^{\sqrt{\varepsilon^*+1}}$ be the single-layer potential associated with the kernel $\Phi\left(\sqrt{1+\varepsilon^*}\,(\,\cdot\,)\right)$.

Definition 2.1. *The scattering coefficient $W_{nm}(D,\varepsilon^*)$ for $n,m \in \mathbb{Z}$ is defined as follows:*

$$W_{nm}(D,\varepsilon^*) = \int_{\partial\Omega} J_n(r_x)\,e^{-in\theta_x}\phi_m(x)\,ds(x)\,, \tag{2.7}$$

where $x = r_x(\cos\theta_x, \sin\theta_x)$ in polar coordinates and the weight function $\phi_m \in L^2(\partial D)$ is such that the pair $(\phi_m, \psi_m) \in L^2(\partial D) \times L^2(\partial D)$ satisfies the following system of integral equations:

$$\begin{cases} S_{\partial D}^{\sqrt{\varepsilon^*+1}}[\phi_m](x) - S_{\partial D}[\psi_m](x) = J_m(r_x)e^{im\theta_x}\,, \\ \frac{\partial}{\partial\nu} S_{\partial D}^{\sqrt{\varepsilon^*+1}}[\phi_m]\,|_-\,(x) - \frac{\partial}{\partial\nu} S_{\partial D}[\psi_m]\,|_+\,(x) = \frac{\partial}{\partial\nu}(J_m(r_x)e^{im\theta_x}). \end{cases} \tag{2.8}$$

Here $+$ and $-$ in the subscripts respectively indicate the limit from outside D and inside D to ∂D along the normal direction, and $\partial/\partial\nu$ denotes the normal derivative.

According to [18, 2], the scattering coefficients $W_{nm}(D,\varepsilon^*)$ are basically the Fourier coefficients of the far-field pattern (scattering amplitude) which is 2π-periodic function in two dimensions. The far-field pattern $A_\infty(\widehat{d},\widehat{x})$, when the incident field is given by $e^{i\widehat{d}\cdot x}$ for a unit vector $\widehat{d}$, is defined to be

$$(u-u^i)(x) = ie^{-\pi i/4}\frac{e^{i|x|}}{\sqrt{8\pi|x|}}A_\infty(\widehat{d},\widehat{x}) + O(|x|^{-\frac{3}{2}}) \quad \text{as } |x| \to \infty,$$

with $\widehat{x} := x/|x|$. We have, recalling from [18, 2], that

$$W_{nm}(D,\varepsilon^*) = i^{n-m}\mathfrak{F}_{\theta_d,\theta_x}[A_\infty(\widehat{d},\widehat{x})](-m,n), \tag{2.9}$$

where $\widehat{x} = (\cos\theta_x, \sin\theta_x)$ and $\widehat{d} = (\cos\theta_d, \sin\theta_d)$ are in polar coordinates and $\mathfrak{F}_{\theta_d,\theta_x}[A_\infty(\widehat{d},\widehat{x})](m,n)$ denotes the (m,n)-th Fourier coefficient of the far-field pattern $A_\infty(\widehat{d},\widehat{x})$, under the Fourier basis functions $\{e^{i(m\theta_d+n\theta_x)}\}_{n,m=-\infty}^{\infty}$.

Our first objective is then to work out an explicit relation between the far-field pattern and the contrast ε^* so as to obtain the behavior of the scattering coefficients when ε^* is large.

In view of (2.4), we introduce the following operator for the subsequent analysis.

Definition 2.2. *The operator $\widetilde{K}_D : L^2(D) \to L^2(D)$ is defined by*

$$\widetilde{K}_D[\phi](x) = \int_D \Phi(x-y)\phi(y)\,dy\,, \quad \text{for } x \in D \text{ and } \phi \in L^2(D)\,; \tag{2.10}$$

whereas, the operator $\widetilde{\widetilde{K}}_D : L^2(D) \to L^\infty(\mathbb{R}^2)$ is given by

$$\widetilde{\widetilde{K}}_D[\phi](x) = \int_D \Phi(x-y)\phi(y)\,dy\,, \quad \text{for } x \in \mathbb{R}^2 \text{ and } \phi \in L^2(D)\,. \tag{2.11}$$

It is easy to see from the definition of $\widetilde{K}_D$ and the Rellich lemma that $\widetilde{K}_D$ is a compact operator. However, it is worth emphasizing that $\widetilde{K}_D$ is not a normal operator in $L^2(D)$. Therefore, it is not unitary equivalent to a multiplicative operator. With Definition 2.2, we can rewrite (2.4) as

$$(I + \varepsilon^* \widetilde{K}_D)[u](x) = u^i(x)\,, \quad \forall x \in D\,. \tag{2.12}$$

By the Fredholm theory [19] and the injectivity of operator $I + \varepsilon^* \widetilde{K}_D$ (see, e.g., [20]), we know

$$u = (I + \varepsilon^* \widetilde{K}_D)^{-1}[u^i]\,. \tag{2.13}$$

From the well-known fact that

$$\Phi(x-y) = -\frac{i}{4} H_0^{(1)}(|x-y|) = -ie^{-\pi i/4} \frac{e^{i|x| - i\widehat{x}\cdot y}}{\sqrt{8\pi|x|}} + O(|x|^{-\frac{3}{2}}) \quad \text{as} \quad |x| \to \infty\,, \tag{2.14}$$

we have

$$u^s(x) = -\varepsilon^* \int_D \Phi(x-y) u(y)\, dy = i\varepsilon^* e^{-\pi i/4} \frac{e^{i|x|}}{\sqrt{8\pi|x|}} \int_D e^{-i\widehat{x}\cdot y} u(y)\, dy + O(|x|^{-\frac{3}{2}}) \quad \text{as} \quad |x| \to \infty. \tag{2.15}$$

Therefore, the far-field of the scattered field can be written as

$$A_\infty(\theta_d, \theta_x) := A_\infty(\widehat{d}, \widehat{x}) = \varepsilon^* \int_D e^{-i\widehat{x}\cdot y} u(y) dy\,. \tag{2.16}$$

Recall the following well-known Jacobi-Anger identity [21] for any unit vector $\widehat{d}$,

$$e^{-i\widehat{d}\cdot x} = \sum_{n=-\infty}^{\infty} (-i)^n J_n(r) e^{in(\theta_d - \theta)} \tag{2.17}$$

for $x = (r, \theta)$ in polar coordinates. Using (2.17) and taking the Fourier transform with respect to θ_x, we get

$$\mathfrak{F}_{\theta_x}[A_\infty](n) = (-i)^n \varepsilon^* \langle J_n(r) e^{in\theta}, u\rangle_{L^2(D)} = i^{-n} \left\langle J_n(r) e^{in\theta}, (\varepsilon^{*-1} + \widetilde{K}_D)^{-1}[u^i] \right\rangle_{L^2(D)}\,. \tag{2.18}$$

Now using $u^i(x) = e^{i\widehat{d}\cdot x}$, it follows from (2.9) and (2.17)-(2.18) that the following proposition holds:

Proposition 2.3. *For a domain D and a contrast ε^*, the scattering coefficient $W_{nm}(D, \varepsilon^*)$ for $n, m \in \mathbb{Z}$ can be written in the following form*

$$W_{nm}(D, \varepsilon^*) = i^{(n-m)} \mathfrak{F}_{\theta_d, \theta_x}[A(\theta_d, \theta_x)](-m, n) = \left\langle J_n(r) e^{in\theta}, (\varepsilon^{*-1} + \tilde{K}_D)^{-1}[J_m(r) e^{im\theta}] \right\rangle_{L^2(D)}\,, \tag{2.19}$$

where $\tilde{K}_D$ is defined by (2.10).

The expression (2.19) of the scattering coefficients W_{nm} will be fundamental to the analysis of the behavior of W_{nm} with respect to ε^*.

Using (2.19), we can readily obtain an *a priori* estimate for the coefficients W_{nm}. Let us first recall the following facts on Schatten-von Neumann ideals; see, for example, [22]. Given a Hilbert space H, we let $\mathfrak{B}(H)$ to be the set of bounded operators on H. We denote by $S_\infty(H)$ the closed two-sided ideal of compact operators in $\mathfrak{B}(H)$. For $K \in S_\infty$ and $k \in \mathbb{N}$, let the k-th singular number $s_k(K)$ be defined as the k-th eigenvalue of $|K| = \sqrt{K^*K}$ ordered in descending order of magnitude and being repeated according to its multiplicity, written as $s_k(K) := \lambda_k(|K|)$. Now, for $0 < p \le \infty$, we shall often write the following Schatten-von Neumann quasi-norms (which are norms if $1 \le p \le \infty$) as follows:

$$||K||_{S_p(H)} := \left(\sum_{k=1}^{\infty} s_k(K)^p \right)^{1/p} \text{ for } p < \infty\,; \quad ||K||_{S_\infty(H)} := ||K||_H\,, \tag{2.20}$$

whenever they are finite. Now let the Schatten-von Neumann quasi-normed operator ideal $S_p(H)$ be defined by

$$S_p(H) := \left\{ K \in S_\infty \,:\, ||K||_{S_p(H)} < \infty \right\} . \tag{2.21}$$

Note that with this convention, $S_1(H)$ is the well-known trace class, $S_2(H)$ is the usual Hilbert-Schmidt class, and $S_\infty(H)$ is the usual class of compact operators in H. Moreover, if $H = L^2(D)$ and $K \in S_2(H)$ is the integral operator defined by

$$K[f](x) = \int_D K(x,y) f(y)\, dy, \quad \text{for } x \in D \text{ and } f \in L^2(D)\,, \tag{2.22}$$

then it holds that

$$||K||^2_{S_2(L^2(D))} = \int_D \int_D |K(x,y)|^2\, dx\, dy, \tag{2.23}$$

which is always well-defined for any $K \in S_2(L^2(D))$. We refer the reader to, for example, [22] for more properties concerning the Schatten-von Neumann ideals.

For a compact operator K, let $\sigma(K) := \{\lambda \in \mathbb{C} |\, \lambda - K \text{ is singular}\}$ denote its spectrum and $(z-K)^{-1}$ its resolvent operator whenever $z \in \mathbb{C}\backslash\sigma(K)$. Now, we have the following resolvent estimate [23].

Proposition 2.4. *For $0 < p < \infty$ and $K \in S_p(H)$, we have the following estimate for the resolvent operator $(z-K)^{-1}$ that*

$$\left|\left| (z-K)^{-1} \right|\right|_H \le \frac{1}{d(z,\sigma(K))} \exp\left(a_p \frac{||K||^p_{S_p(H)}}{d(z,\sigma(K))^p} + b_p \right), \tag{2.24}$$

where a_p, b_p are two constants depending on p and $d(z,\sigma(K))$ is defined by

$$d(z,\sigma(K)) := \inf_{\lambda\in\sigma(K)} |z-\lambda|\,. \tag{2.25}$$

Now we can apply Proposition 2.4 to get an estimate for $W_{nm}(D,\varepsilon^*)$. In fact, with the logarithmic type singularity of the function $H_0^{(1)}$, we readily obtain that

$$||\tilde{K}_D||^2_{S_2(L^2(D))} = \int_D \int_D |H_0^{(1)}(|x-y|)|^2\, dx\, dy < C\,(1+R)^4\,(1+\log R)^2 < \infty, \tag{2.26}$$

whenever $D \subset B(0,R)$, and hence $\tilde{K}_D \in S_2$. Therefore, using the Cauchy-Schwartz inequality and applying (2.24) for $H = L^2(D)$ to (2.19), together with the following well-known asymptotic expression of J_m for large m [24, pp. 365-366],

$$J_m(z) \Big/ \frac{1}{\sqrt{2\pi m}} \left(\frac{ez}{2m}\right)^m \to 1 \quad \text{as } m \to \infty\,, \tag{2.27}$$

we readily obtain the following inequality (using that $a_2 = 1/2, b_2 = 1/2$ if $p = 2$ [25]):

$$\begin{aligned}
|W_{nm}(D,\varepsilon^*)| &= \left| \left\langle J_n(r)e^{in\theta}, (\varepsilon^{*-1} + \tilde{K}_D)^{-1}[J_m(r)e^{im\theta}] \right\rangle_{L^2(D)} \right| \\
&\le \left|\left| (\varepsilon^{*-1} + \tilde{K}_D)^{-1} \right|\right|_{L^2(D)} \left|\left| J_n(r)e^{in\theta} \right|\right|_{L^2(D)} \left|\left| J_m(r)e^{im\theta} \right|\right|_{L^2(D)} \\
&\le \frac{1}{d(-\varepsilon^{*-1}, \sigma(\tilde{K}_D))} \exp\left(\frac{||\tilde{K}_D||^2_{S_2(L^2(D))}}{d(-\varepsilon^{*-1}, \sigma(\tilde{K}_D))^2} + \frac{1}{2} \right) \left|\left| J_n(r)e^{in\theta} \right|\right|_{L^2(D)} \left|\left| J_m(r)e^{im\theta} \right|\right|_{L^2(D)} \\
&\le \frac{1}{d(-\varepsilon^{*-1}, \sigma(\tilde{K}_D))} \exp\left(\frac{C_{1,R}}{d(-\varepsilon^{*-1}, \sigma(\tilde{K}_D))^2} + \frac{1}{2} \right) \frac{C_{2,R}^{|m|+|n|}}{|m|^{|m|}|n|^{|n|}},
\end{aligned}$$

where $C_{i,R}\,(i = 1,2)$ are some constants, which depend only on the radius R such that $D \subset B(0,R)$. We summarize the above result in the following theorem.

Corollary 2.5. *For a given domain D and a contrast ε^*, we have the following estimate for the scattering coefficient $W_{nm}(D,\varepsilon^*)$, for $n,m\in\mathbb{Z}$,*

$$|W_{nm}(D,\varepsilon^*)|\leq \frac{1}{d(-\varepsilon^{*-1},\sigma(\tilde{K}_D))}\exp\left(\frac{C_{1,R}}{d(-\varepsilon^{*-1},\sigma(\tilde{K}_D))^2}+\frac{1}{2}\right)\frac{C_{2,R}^{|m|+|n|}}{|m|^{|m|}|n|^{|n|}}\,. \tag{2.28}$$

From Corollary 2.5, we foresee that the magnitude of W_{nm} may grow as ε^* increases, and becomes a very large value as ε^{*-1} is close to the spectrum of the operator $\tilde{K}_D$.

2.1. The case of a circular domain

Now, we consider the operator $\tilde{K}_D$ for a circular domain, i.e., when $D=B(0,R)$. In this case, the operator $\tilde{K}_D$ becomes more explicit. Actually, from Graf's formula [21], we have for $|x|\neq|y|$ that

$$H_0^{(1)}(|x-y|)=\sum_{m=-\infty}^{\infty}\chi_{\{|x|<|y|\}}J_m(|x|)e^{-im\theta_x}H_m^{(1)}(|y|)e^{im\theta_y}+\chi_{\{|x|>|y|\}}H_m^{(1)}(|x|)e^{-im\theta_x}J_m(|y|)e^{im\theta_y}\,.$$

Therefore, for all $f\in L^2(D)$, the operator $\widetilde{K}_D$ can be written as

$$\begin{aligned}\widetilde{K}_D[f](y)=-\frac{i}{4}\sum_{m=-\infty}^{\infty}\Big[&\langle J_m(r)e^{im\theta},f\rangle_{D\bigcap B(0,|y|)}H_m^{(1)}(|y|)e^{im\theta_y}\\&+\langle\overline{H_m^{(1)}(r)}e^{im\theta},f\rangle_{D\setminus\overline{B(0,|y|)}}J_m(|y|)e^{im\theta_y}\Big]\,.\end{aligned}$$

The above expression of $\tilde{K}_D$ will be helpful to investigate the behavior of $\tilde{K}_D$ and W_{nm}. Before we continue our discussion on the operator $\tilde{K}_D$, we shall first define some operators.

Definition 2.6. *Given an integer $m\in\mathbb{Z}$, the operators $\widetilde{K}_m^{(i)}:L^2((0,R),r\,dr)\to L^2((0,R),r\,dr)$ for $i=1,2$ are defined as*

$$\widetilde{K}_m^{(i)}[\phi](h)=-\frac{i}{4}\bigg(\int_0^h rJ_m(r)\phi(r)dr\bigg)H_m^{(i)}(h)-\frac{i}{4}\bigg(\int_h^R rH_m^{(i)}(r)\phi(r)dr\bigg)J_m(h) \tag{2.29}$$

for $h\in(0,R)$ and $\phi\in L^2((0,R),r\,dr)$, and their extensions $\widetilde{\widetilde{K}}_m^{(i)}:L^2((0,R),r\,dr)\to L^\infty((0,+\infty))$ for $i=1,2$ as

$$\widetilde{\widetilde{K}}_m^{(i)}[\phi](h)=-\frac{i}{4}\bigg(\int_0^h rJ_m(r)\phi(r)dr\bigg)H_m^{(i)}(h)-\frac{i}{4}\bigg(\int_h^R rH_m^{(i)}(r)\phi(r)dr\bigg)J_m(h) \tag{2.30}$$

for $h\in(0,+\infty)$ and $\phi\in L^2((0,R),r\,dr)$.

With this notion, we can readily see that if $f\in L^2(D)$ has the form $f=\phi(r)e^{im\theta}$, then we have in polar coordinates by the orthogonality of $\{e^{im\theta}\}_{m\in\mathbb{Z}}$ on $L^2(\mathbb{S}^1)$ that

$$\begin{aligned}\widetilde{K}_D[f](h,\theta)&=-\frac{i}{4}\bigg(\int_0^h rJ_m(r)\phi(r)dr\bigg)H_m^{(1)}(h)e^{im\theta}-\frac{i}{4}\bigg(\int_h^R rH_m^{(1)}(r)\phi(r)dr\bigg)J_m(h)e^{im\theta}\\&=\widetilde{K}_m^{(1)}[\phi](h)e^{im\theta}\,,\end{aligned} \tag{2.31}$$

and $\widetilde{K}_D^*[f](h,\theta)=\widetilde{K}_m^{(2)}[\phi](h)e^{im\theta}$. Furthermore, we can directly see that $\sigma(\tilde{K}_m^{(2)})=\overline{\sigma(\tilde{K}_m^{(1)})}$. Moreover, using the following relations for all $m\in\mathbb{Z}$,

$$J_{-m}(z)=(-1)^mJ_m(z)\quad\text{ and }\quad H_{-m}^{(1)}(z)=(-1)^mH_m^{(1)}(z), \tag{2.32}$$

we immediately infer the properties for the integral operators:

$$\widetilde{K}^{(i)}_{-m} = \widetilde{K}^{(i)}_{m} \quad \text{and} \quad \widetilde{\widetilde{K}}^{(i)}_{-m} = \widetilde{\widetilde{K}}^{(i)}_{m} \,. \tag{2.33}$$

Substituting (2.31) into Proposition 2.3, we obtain the following simplified expressions of the scattering coefficients when $D = B(0, R)$.

Proposition 2.7. *For a domain $D = B(0, R)$ for some $R > 0$ and a contrast value ε^*, the scattering coefficient $W_{nm}(D, \varepsilon^*)$, $n, m \in \mathbb{Z}$, can be written in the following form*

$$W_{nm}(D, \varepsilon^*) = \delta_{nm} \left\langle J_n, \left(\varepsilon^{*-1} + \tilde{K}^{(1)}_m\right)^{-1} [J_m] \right\rangle_{L^2((0,R), r\,dr)} , \tag{2.34}$$

where δ_{nm} is the Kronecker symbol.

As a consequence of Proposition 2.7, we easily see that $W_{nm} = 0$ for $n \neq m$. Moreover, we readily have the following *a priori* estimate for the coefficients W_{nm} by the same arguments as those in Corollary 2.5. In order to obtain the desired estimate, we consider the asymptotic expression of Y_m as $m \to \infty$ [24, pp. 365-366]:

$$Y_m(z) \Big/ \sqrt{\frac{2}{\pi m}} \left(\frac{ez}{2m}\right)^{-m} \to 1 \,. \tag{2.35}$$

Together with (2.27) and the logarithmic type singularity of Y_0, we have from the definitions of $\widetilde{K}^{(i)}_m$ for $i = 1, 2$ in (2.29) that

$$||\widetilde{K}^{(i)}_m)||^2_{S_2(L^2((0,R), r\,dr))} \leq C_m \left(1 + R\right)^4 \left(1 + \log R\right)^2 < \infty \,. \tag{2.36}$$

Consequently, following the same arguments as the ones for (2.28), we arrive at the estimate:

$$\begin{aligned} |W_{nm}(D, \varepsilon^*)| &= \delta_{nm} \left| \left\langle J_n, \left(\varepsilon^{*-1} + \tilde{K}^{(1)}_m\right)^{-1} [J_m] \right\rangle_{L^2((0,R), r\,dr)} \right| \\ &\leq \delta_{nm} \frac{1}{d\left(-\varepsilon^{*-1}, \sigma(\tilde{K}^{(1)}_m)\right)} \exp\left(\frac{C_m C_{1,R}}{d\left(-\varepsilon^{*-1}, \sigma(\tilde{K}^{(1)}_m)\right)^2} + \frac{1}{2} \right) \frac{C_{2,R}^{|m|+|n|}}{|m|^{|m|} |n|^{|n|}}, \end{aligned}$$

where C_m is a constant depending only on m and $C_{i,R}, i = 1, 2$, are constants only depending on the radius R such that $D \subset B(0, R)$.

Corollary 2.8. *For a circular domain $D = B(0, R)$ and a contrast ε^*, we have the following estimate for the scattering coefficient $W_{nm}(D, \varepsilon^*)$, for $n, m \in \mathbb{Z}$,*

$$|W_{nm}(D, \varepsilon^*)| \leq \delta_{nm} \frac{1}{d\left(-\varepsilon^{*-1}, \sigma(\tilde{K}^{(1)}_m)\right)} \exp\left(\frac{C_m C_{1,R}}{d\left(-\varepsilon^{*-1}, \sigma(\tilde{K}^{(1)}_m)\right)^2} + \frac{1}{2} \right) \frac{C_{2,R}^{|m|+|n|}}{|m|^{|m|} |n|^{|n|}} \,. \tag{2.37}$$

In the next section we perform a sensitivity analysis of the scattering coefficients in order to obtain a quantitative description of what piece of information is provided by the scattering coefficients of different orders.

3. Sensitivity analysis of the scattering coefficients for a given contrast

In this section, for a given contrast ε^*, we calculate the shape derivative $\mathcal{D}W_{nm}(D,\varepsilon^*)[h]$ of the scattering coefficient $W_{nm}(D,\varepsilon^*)$ along the variational direction $h \in \mathcal{C}^1(\partial D)$ when ∂D is of class $\mathcal{C}^2$. From the shape derivative, we will clearly understand what piece of information is provided by the scattering coefficients of different orders, and how the knowledge of the scattering coefficients is related to the resolution of the reconstructed shapes.

Let us first recall the definition of the shape derivative of a function $\mathcal{F}[D]$, where the argument of the function is a domain D, which is essential for our sensitivity analysis later in this section. For a given bounded $\mathcal{C}^2$-domain D in $\mathbb{R}^2$, let D^δ be its δ-perturbation in the variational direction $h \in \mathcal{C}^1(\partial D)$, i.e.,

$$\partial D^\delta := \left\{ \tilde{x} = x + \delta h(x)\nu(x) \,:\, x \in \partial D \right\}, \tag{3.1}$$

where $\nu(x)$ is the outward unit normal to ∂D. Then the shape derivative of a function $\mathcal{F}[D]$ in the variational direction $h \in \mathcal{C}^1(\partial D)$, denoted as $\mathcal{D}\mathcal{F}(D)$, is defined to satisfy the following relationship:

$$\mathcal{F}[D^\delta] = \mathcal{F}[D] + \delta\, \mathcal{D}\mathcal{F}(D)[h] + O(\delta^2)\,. \tag{3.2}$$

Before going to the sensitivity analysis, we consider now the inclusion of the operators and their spectra. To do so, we define the following inclusion maps.

Definition 3.1. *For a given domain D, suppose that the bounded linear operator $\tilde{K}_D \in \mathfrak{B}\left(L^2(D)\right)$ is defined as in* (2.10)*. Consider any domain $\widehat{D}$ such that $D \subset \widehat{D}$, we shall often write $\iota(\tilde{K}_D) \in \mathfrak{B}\left(L^2(\widehat{D})\right)$ as the following operator:*

$$\iota(\tilde{K}_D)\,[f]\,(x) = \tilde{\tilde{K}}_D\,[\chi_D f]\,(x) \quad \text{ for any } f \in L^2(\widehat{D})\,, \tag{3.3}$$

where χ_D is the characteristic function of D. Likewise, for a given radius $R > 0$, assume the bounded linear operators $\tilde{K}_m^{(i)} \in \mathfrak{B}\left(L^2((0,R), r\,dr)\right)$ $(m \in \mathbb{Z},\, i = 1,2)$, which are defined in (2.29)*. Then we write*

$$\iota(\tilde{K}_m^{(i)})\,[f]\,(x) = \tilde{\tilde{K}}_m^{(i)}\left[\chi_{(0,R)} f\right](x) \quad \text{ for any } f \in L^2((0,\widehat{R}), r\,dr)\,. \tag{3.4}$$

Then the operators $\iota(\tilde{K}_D)$ and $\iota(\tilde{K}_m^{(i)})$, $i = 1,2$, are compact on $L^2((0,\widehat{R}), r\,dr)$. Moreover, we have the following relations between the spectra of $\tilde{K}_D$ and $\iota(\tilde{K}_D)$, as well as between $\tilde{K}_m^{(i)}$ and $\iota(\tilde{K}_m^{(i)})$ for $m \in \mathbb{Z}$, $i = 1,2$.

Lemma 3.2. *Let $\tilde{K}_D$ and $\iota(\tilde{K}_D)$ be defined as in* (2.10) *and* (3.3)*, respectively. Then, the following simple relationship between the spectra of $\tilde{K}_D$ and $\iota(\tilde{K}_D)$ holds:*

$$\sigma(\iota(\tilde{K}_D)) = \sigma(\tilde{K}_D) \bigcup \{0\}\,. \tag{3.5}$$

Likewise, for $m \in \mathbb{Z}$, $i = 1,2$, we have

$$\sigma(\iota(\tilde{K}_m^{(i)})) = \sigma(\tilde{K}_m^{(i)}) \bigcup \{0\}\,. \tag{3.6}$$

Proof. For a given λ, suppose that the pair (λ, e_λ) is an eigenpair of $\tilde{K}_D$ over $L^2(D)$. If $\lambda \neq 0$, we denote by $\widetilde{e_\lambda} \in L^2(\widehat{D})$ the following function

$$\widetilde{e_\lambda} := \frac{1}{\lambda} \widetilde{\widetilde{K_D}}[e_\lambda]\,. \tag{3.7}$$

If $\lambda = 0$, we write $\widetilde{e_\lambda} \in L^2(\widehat{D})$ as the extension by zero of the function e_λ outside the domain D, i.e.,

$$\widetilde{e_\lambda}(x) := \begin{cases} e_\lambda(x) & \text{if } x \in \mathrm{D}\,, \\ 0 & \text{otherwise}\,. \end{cases} \tag{3.8}$$

Then we readily check from the definition of $\iota(\tilde{K}_D)$ that $\iota(\tilde{K}_D)[\widetilde{e_\lambda}] = \lambda\widetilde{e_\lambda}$ and hence the pair $(\lambda, \widetilde{e_\lambda})$ is an eigenpair of $\iota(\tilde{K}_D)$ over $L^2(\widehat{D})$. As any function $f \in L^2(\widehat{D}\backslash D)$ is a zero eigenfunction of $\iota(\tilde{K}_D)$, hence we know $\sigma(\tilde{K}_D)\bigcup\{0\} \subset \sigma(\iota(\tilde{K}_D))$.

Conversely, if a pair $(\lambda, \widetilde{e_\lambda})$ is an eigenpair of $\iota(\tilde{K}_D)$ over $L^2(\widehat{D})$, then, by writing $e_\lambda := \widetilde{e_\lambda}\,|_D$, it is easy to see form the definition of $\tilde{K}_D$ that (λ, e_λ) is an eigenpair of $\tilde{K}_D$. Hence, $\sigma(\iota(\tilde{K}_D)) \subset \sigma(\tilde{K}_D)$. The proof of $\sigma(\iota(\tilde{K}_m^{(i)})) = \sigma(\tilde{K}_m^{(i)})\bigcup\{0\}$ is the same. □

Lemma 3.2 and the Fredholm alternative yield that $\varepsilon^{*-1} + \iota(\tilde{K}_D)$ is invertible over $L^2(\widehat{D})$ if and only if $\varepsilon^{*-1} + \tilde{K}_D$ is invertible over $L^2(D)$. Moreover, from the definition, we can show as in section 2 that $\iota(\tilde{K}_D) \in S_2(L^2(\widehat{D}))$ and then apply (2.24) to obtain the following resolvent estimate for $\varepsilon^{*-1} + \iota(\tilde{K}_D)$ that

$$\begin{aligned}\left|\left|\left(\varepsilon^{*-1} + \iota(\tilde{K}_D)\right)^{-1}\right|\right|_{L^2(\widehat{D})} &\leq \frac{1}{d\left(-\varepsilon^{*-1}, \sigma(\iota(\tilde{K}_D))\right)} \exp\left(\frac{C_{1,R}}{d\left(-\varepsilon^{*-1}, \sigma(\iota(\tilde{K}_D))\right)^2} + \frac{1}{2}\right) \\ &= \frac{1}{d\left(-\varepsilon^{*-1}, \sigma(\tilde{K}_D)\right)} \exp\left(\frac{C_{1,R}}{d\left(-\varepsilon^{*-1}, \sigma(\tilde{K}_D)\right)^2} + \frac{1}{2}\right). \end{aligned} \tag{3.9}$$

Here the last equality comes from Lemma 3.2 and the fact that $\sigma(\widetilde{K}_D)$ must have zero as its accumulation point, since $L^2(D)$ is infinite dimensional. The above argument also applies to the operators $\iota(\tilde{K}_m^{(i)})$ for $m \in \mathbb{Z}, i = 1, 2$, where the resolvent estimate reads

$$\left|\left|\left(\varepsilon^{*-1} + \iota(\tilde{K}_m^{(i)}))\right)^{-1}\right|\right|_{L^2((0,\widehat{R}),r\,dr)} \leq \frac{1}{d\left(-\varepsilon^{*-1}, \sigma(\tilde{K}_m^{(1)})\right)} \exp\left(\frac{C_m C_{1,R}}{d\left(-\varepsilon^{*-1}, \sigma(\tilde{K}_m^{(1)})\right)^2} + \frac{1}{2}\right). \tag{3.10}$$

Furthermore, we can easily recover the relationship between $\iota(\widetilde{K}_{B(0,R)})$ and $\iota(\tilde{K}_m^{(i)})$ for any D such that $B(0,R) \subset D$ from their definitions. In fact, for any $f \in L^2(D)$ in the form $f = \phi(r)e^{im\theta}$, where $(r,\theta) \in D$, we have in polar coordinates that

$$\iota(\widetilde{K}_{B(0,R)})[f](h,\theta) = \iota(\widetilde{K}_m^{(1)})[\phi](h)e^{im\theta}, \quad \iota(\widetilde{K}^*_{B(0,R)})[f](h,\theta) = \iota(\widetilde{K}_m^{(2)})[\phi](h)e^{im\theta}, \tag{3.11}$$

where the operators $\iota(\widetilde{K}_m^{(i)})$ for $m \in \mathbb{Z}, i = 1, 2$, are the extensions to $L^2((0,\widehat{R}_\theta), r\,dr)$ with the radii $\widehat{R}_\theta$ being defined as $\widehat{R}_\theta := \sup\{r : (r,\theta) \in D\}$ for different $\theta \in [0, 2\pi]$. Although the extensions $\iota(\widetilde{K}_m^{(i)})$ are now different for different angles θ, no difficulty will arise in understanding the properties of $\iota(\widetilde{K}_{B(0,R)})$ via estimating $\iota(\widetilde{K}_m^{(1)})$, since the conclusions of Lemma 3.2 and (3.10) do not depend on the choice of $\widehat{R}$ and thus can be applied to different choices of radii.

From now on, we will no longer distinguish between the operators $\tilde{K}_D$ and $\iota(\tilde{K}_D)$ whenever there is no ambiguity, and by an abuse of notation, we denote both operators by $\tilde{K}_D$, likewise for the operators $\tilde{K}_m^{(i)}$ and $\iota(\tilde{K}_m^{(i)})$ for $m \in \mathbb{Z}, i = 1, 2$.

Then we move to our main focus of this subsection, which is to obtain the shape derivative of the scattering coefficients for a domain D along a perturbation $h \in \mathcal{C}^1(\partial D)$. Now let ε^* be given. For any bounded $\mathcal{C}^2$-domain D in $\mathbb{R}^2$, let D^δ be a δ-perturbation of D along the variational direction $h \in \mathcal{C}^1(\partial D)$ as in (3.1). For such perturbations of the domain D, we investigate the difference between $W_{nm}(D^\delta, \varepsilon^*)$ and $W_{nm}(D, \varepsilon^*)$. We first estimate the difference $\tilde{K}_{D^\delta} - \tilde{K}_D$, where both operators $\tilde{K}_{D^\delta}$ and $\tilde{K}_D$ are regarded as the extended operators on $L^2\left(D^\delta \bigcup D\right)$. Indeed, from the fact that the singularity type of the function $H_0^{(1)}$ is logarithmic, there exists a constant C_R depending only on the radius R such that the estimate

$$||\tilde{K}_{D^\delta} - \tilde{K}_D||_{L^2(B(0,R))} \leq C_R\,\delta \tag{3.12}$$

holds for δ small enough with R being such that $D \Subset B(0,R)$. Therefore, we can repeatedly apply the following resolvent identities

$$\left(\varepsilon^{*-1}+\tilde{K}_{D^\delta}\right)^{-1}-\left(\varepsilon^{*-1}+\tilde{K}_{D}\right)^{-1} = \left(\varepsilon^{*-1}+\tilde{K}_{D^\delta}\right)^{-1}(\tilde{K}_D-\tilde{K}_{D^\delta})\left(\varepsilon^{*-1}+\tilde{K}_{D}\right)^{-1} \quad (3.13)$$

$$= \left(\varepsilon^{*-1}+\tilde{K}_{D}\right)^{-1}(\tilde{K}_D-\tilde{K}_{D^\delta})\left(\varepsilon^{*-1}+\tilde{K}_{D^\delta}\right)^{-1} \quad (3.14)$$

to obtain the following expression of the difference of scattering coefficients for any $n,m\in\mathbb{Z}$,

$$\begin{aligned}
& W_{nm}(D^\delta,\varepsilon^*)-W_{nm}(D,\varepsilon^*)\\
= & \left\langle J_n(r)e^{in\theta},\left[\left(\varepsilon^{*-1}+\tilde{K}_{D^\delta}\right)^{-1}-\left(\varepsilon^{*-1}+\tilde{K}_{D}\right)^{-1}\right][J_m(r)e^{im\theta}]\right\rangle_{L^2(D)}\\
& +\left\langle\left(\varepsilon^{*-1}+\tilde{K}^*_{D^\delta}\right)^{-1}[J_n(r)e^{in\theta}],\mathrm{sgn}(h)\,J_m(r)e^{im\theta}\right\rangle_{L^2(D\bigcup D^\delta\setminus D\bigcap D^\delta)}\\
= & -\left\langle\left(\varepsilon^{*-1}+\tilde{K}^*_{D}\right)^{-1}[J_n(r)e^{in\theta}],(\tilde{K}_{D^\delta}-\tilde{K}_D)\left(\varepsilon^{*-1}+\tilde{K}_{D}\right)^{-1}[J_m(r)e^{im\theta}]\right\rangle_{L^2(D)}\\
& +\left\langle\left(\varepsilon^{*-1}+\tilde{K}^*_{D}\right)^{-1}[J_n(r)e^{in\theta}],\mathrm{sgn}(h)\,J_m(r)e^{im\theta}\right\rangle_{L^2(D\bigcup D^\delta\setminus D\bigcap D^\delta)}+O(\delta^2), \quad (3.15)
\end{aligned}$$

where the last equality comes from the resolvent identities and (3.12). Now for any L^1 function f, considering the fact that the shape derivative of the integral

$$I(D)=\int_D f(x)dx \quad (3.16)$$

is given by the following boundary integral

$$\mathcal{D}\,I(D)[h]=\int_{\partial D} f(x)h(x)\,ds(x)\,, \quad (3.17)$$

we have for $x\in D\bigcup D^\delta$ and $\phi\in L^2(D\bigcup D^\delta)$ that

$$\begin{aligned}
(\tilde{K}_{D^\delta}-\tilde{K}_D)[\phi](x) &= -\frac{i}{4}\int_{(D\bigcup D^\delta)\setminus(D\bigcap D^\delta)}\mathrm{sgn}(h)\,H_0^{(1)}(|x-y|)\phi(y)dy\\
&= -\delta\frac{i}{4}\int_{\partial D}H_0^{(1)}(|x-y|)h(y)\phi(y)\,ds(y)+O(\delta^2)\,. \quad (3.18)
\end{aligned}$$

Therefore, by substituting the above expression into (3.15), a direct expansion of the integral together with Fubini's theorem yields the following expression for the first term in (3.15):

$$\begin{aligned}
& -\left\langle\left(\varepsilon^{*-1}+\tilde{K}^*_{D}\right)^{-1}[J_n(r)e^{in\theta}],(\tilde{K}_{D^\delta}-\tilde{K}_D)\left(\varepsilon^{*-1}+\tilde{K}_{D}\right)^{-1}[J_m(r)e^{im\theta}]\right\rangle_{L^2(D)}\\
= & \ \delta\frac{i}{4}\int_D\int_{\partial D}H_0^{(1)}(|x-y|)h(y)\left[\left(\varepsilon^{*-1}+\tilde{K}_{D}\right)^{-1}[J_m(r)e^{im\theta}]\right](y)\,dy\overline{\left[\left(\varepsilon^{*-1}+\tilde{K}^*_{D}\right)^{-1}[J_n(r)e^{in\theta}]\right](x)}\,dx\\
& +O(\delta^2)\\
= & -\delta\left\langle\overline{\left[\left(\varepsilon^{*-1}+\tilde{K}_{D}\right)^{-1}[J_m(r)e^{im\theta}]\right]}\left[\tilde{K}^*_D\left(\varepsilon^{*-1}+\tilde{K}^*_{D}\right)^{-1}[J_n(r)e^{in\theta}]\right],h\right\rangle_{L^2(\partial D)}+O(\delta^2). \quad (3.19)
\end{aligned}$$

Likewise, for the second term in (3.15), we derive that

$$\begin{aligned}
& \left\langle\left(\varepsilon^{*-1}+\tilde{K}^*_{D}\right)^{-1}[J_n(r)e^{in\theta}],\mathrm{sgn}(h)\,J_m(r)e^{im\theta}\right\rangle_{L^2(D\bigcup D^\delta\setminus D\bigcap D^\delta)}\\
= & \ \delta\left\langle\overline{\left[\left(\varepsilon^{*-1}+\tilde{K}_{D}\right)^{-1}[J_m(r)e^{im\theta}]\right]}\left[J_n(r)e^{in\theta}\right],h\right\rangle_{L^2(\partial D)}+O(\delta^2). \quad (3.20)
\end{aligned}$$

Therefore, combining the above two estimates shows that

$$\begin{aligned} & W_{nm}(D^\delta,\varepsilon^*) - W_{nm}(D,\varepsilon^*) \\ = \;& \delta\varepsilon^{*-1}\left\langle \overline{\left[\left(\varepsilon^{*-1}+\tilde{K}_D\right)^{-1}[J_m(r)e^{im\theta}]\right]}\left[\left(\varepsilon^{*-1}+\tilde{K}_D^*\right)^{-1}[J_n(r)e^{in\theta}]\right], h\right\rangle_{L^2(\partial D)} \\ & + O(\delta^2)\,. \end{aligned} \tag{3.21}$$

Hence, if we define the following $L^2(\partial D)$-duality gradient function $\nabla W_{nm}(D,\varepsilon^*)$ of the form of

$$\nabla W_{nm}(D,\varepsilon^*) := \varepsilon^{*-1}\overline{\left[\left(\varepsilon^{*-1}+\tilde{K}_D\right)^{-1}[J_m(r)e^{im\theta}]\right]}\left[\left(\varepsilon^{*-1}+\tilde{K}_D^*\right)^{-1}[J_n(r)e^{in\theta}]\right], \tag{3.22}$$

then the shape derivative of the scattering coefficient $W_{nm}(D,\varepsilon^*)$ along the variational direction h is given by

$$\mathcal{D}\,W_{nm}(\varepsilon^*,D)[h] = \langle \nabla W_{nm}(\varepsilon^*,D), h\rangle_{L^2(\partial D)}\,. \tag{3.23}$$

In particular, for the case where D is a circular domain $D = B(0,R)$, we have from the decomposition of the operator $\tilde{K}_D$ the following simple expression of $\nabla W_{nm}(D,\varepsilon^*)$:

$$\nabla W_{nm}(B(0,R),\varepsilon^*) \;=\; \varepsilon^{*-1}\left[\left(\varepsilon^{*-1}+\tilde{K}_m^{(2)}\right)^{-1}[J_m]\right](R)\left[\left(\varepsilon^{*-1}+\tilde{K}_n^{(2)}\right)^{-1}[J_n]\right](R)\,e^{i(n-m)\theta}\,.$$

Consequently, we get that

$$\mathcal{D}\,W_{nm}(B(0,R),\varepsilon^*)[h] \;=\; \varepsilon^{*-1}\left[\left(\varepsilon^{*-1}+\tilde{K}_m^{(1)}\right)^{-1}[J_m]\right](R)\left[\left(\varepsilon^{*-1}+\tilde{K}_n^{(1)}\right)^{-1}[J_n]\right](R)\,\mathfrak{F}_\theta[h](n-m)\,,$$

where $\mathfrak{F}_\theta[h](n-m)$ is the $(n-m)$-th Fourier coefficient of the function h on $L^2(\mathbb{S}^1)$. This gives the following key result on the shape derivative of $W_{nm}(D,\varepsilon^*)$.

Theorem 3.3. *Suppose that $\varepsilon^* > 0$ is given. For any $\mathcal{C}^2$-domain D and $n,m\in\mathbb{Z}$, the shape derivative of the scattering coefficient $W_{nm}(D,\varepsilon^*)$ along the variational direction $h\in L^2(\partial D)$ is given by*

$$\mathcal{D}\,W_{nm}(D,\varepsilon^*)[h] = \langle \nabla W_{nm}(D,\varepsilon^*), h\rangle_{L^2(\partial D)}\,, \tag{3.24}$$

where ∇W_{nm} is defined by

$$\nabla W_{nm}(D,\varepsilon^*) = \varepsilon^{*-1}\overline{\left[\left(\varepsilon^{*-1}+\tilde{K}_D\right)^{-1}[J_m(r)e^{im\theta}]\right]}\left[\left(\varepsilon^{*-1}+\tilde{K}_D^*\right)^{-1}[J_n(r)e^{in\theta}]\right]. \tag{3.25}$$

In particular, if the domain D is a circular domain $D = B(0,R)$, then for any D^δ as a δ-perturbation of D along the variational direction $h\in\mathcal{C}^1(\partial D)$, we have

$$W_{nm}(D^\delta,\varepsilon^*) - W_{nm}(D,\varepsilon^*) = \delta\, C(\varepsilon^*,n,m)\mathfrak{F}_\theta[h](n-m) + O(\delta^2), \tag{3.26}$$

with

$$C(\varepsilon^*,n,m) := \varepsilon^{*-1}\left[\left(\varepsilon^{*-1}+\tilde{K}_m^{(1)}\right)^{-1}[J_m]\right](R)\left[\left(\varepsilon^{*-1}+\tilde{K}_n^{(1)}\right)^{-1}[J_n]\right](R)\,. \tag{3.27}$$

From the above theorem, we obtain in the linearized case that the scattering coefficient W_{nm} gives us precise information about the $(m-n)$-th Fourier mode of the perturbation h.

Therefore, the magnitude of the coefficients W_{nm} and $C(\varepsilon^*,n,m)$ shall be responsible for the resolution in imaging D^δ. Note that the function $C(\varepsilon^*,n,m)$ depends now on the spectra of both $\tilde{K}_m^{(1)}$ and $\tilde{K}_n^{(1)}$. The change and growth of the coefficients W_{nm} and $C(\varepsilon^*,n,m)$ with respect to ε^* will be the main focus of the next section.

4. Asymptotic behaviors of eigenvalues over a circular domain and the phenomenon of super-resolution

In the previous section, we have obtained a relationship between the coefficients W_{nm} of a perturbed circular domain D^δ and the Fourier coefficients of the perturbation h. In this section, we investigate the decay of the eigenvalues of $\tilde{K}_m^{(1)}$ and analyze the behavior with respect to ε^* of W_{nm} and $C(\varepsilon^*, n, m)$ for different values of n and m. Then the phenomenon of super-resolution is explained based on several important implications stated in two main theorems of this section, Theorems 4.6 and 4.9. The former provides the clear asymptotic behavior of the eigenvalues of a related operator, while the latter gives a reason for the stronger sensitivity of the Fourier modes of higher orders when the reciprocal of a contrast comes close to the real parts of the reciprocals of the respective eigenvalues simultaneously. These two theorems combine to provide a justification of the experimentally observed phenomenon about super-resolution for some specific high contrasts as described in the theorems. For this purpose, we first introduce the following Riesz decomposition.

4.1. Riesz decomposition of the operators $\widetilde{K}_D$ and $\tilde{K}_m^{(1)}$

To continue our analysis on the operators $\widetilde{K}_D$ and $\tilde{K}_m^{(1)}$, we first recall the following well-known classical spectral theorem for general compact operators (not necessarily self-adjoint or normal) in a Hilbert space [19].

Proposition 4.1. *Let K be a compact operator on a Hilbert space H, $\sigma(K) := \{\lambda \in \mathbb{C} |\, \lambda - K$ is singular$\}$ be its spectrum, and $\sigma_p(K)$ be its point spectrum consisting of all the eigenvalues of K. Then the following results hold:*

1. *If $\lambda \neq 0$, then we have that $\lambda \in \sigma(K)$ if and only if $\lambda \in \sigma_p(K)$ the point spectrum (Fredholm's alternative).*
2. *For all $\lambda \in \sigma(K)$ such that $\lambda \neq 0$, there exists a smallest m_λ such that $Ker(\lambda - K)^{m_\lambda} = Ker(\lambda - K)^{m_\lambda + 1}$. Denoting the space $Ker(\lambda - K)^{m_\lambda}$ by $E_\lambda := Ker(\lambda - K)^{m_\lambda}$, we have $dim(E_\lambda) < \infty$. Moreover, $Ran(\lambda - K)^{m_\lambda}$ is a closed subspace and $H = Ker(\lambda - K)^{m_\lambda} \bigoplus Ran(\lambda - K)^{m_\lambda}$.*
3. *$\sigma(K)$ is countable and 0 is the only accumulation point of $\sigma(K)$ for $dim(H) = \infty$.*
4. *The map $z \mapsto (z - K)^{-1}$ admits poles at $z \in \sigma(K)$.*

Now we aim to apply the above theorem to $\widetilde{K}_D$, which is compact but not normal, to obtain a spectral decomposition of the operator $\widetilde{K}_D$ and the space $L^2(D)$. In order to do so, we shall assert the following elementary lemma.

Lemma 4.2. *Let $\widetilde{K}_D$ be defined as in* (2.10)*, and $\widetilde{K}_D^*$ be its L^2 adjoint, then we have*

$$\sigma(\widetilde{K}_D) \backslash \sigma_p(\widetilde{K}_D) = \{0\} \quad \text{and } \sigma(\widetilde{K}_D^*) \backslash \sigma_p(\widetilde{K}_D^*) = \{0\}\,.$$

Proof. Let us first consider the operator $\widetilde{K}_D$. From Theorem 4.1, we directly have that

$$\sigma(\widetilde{K}_D) \backslash \{0\} = \sigma_p(\widetilde{K}_D) \backslash \{0\}\,,$$

Therefore, in order to prove our assertion, it suffices to show that $0 \notin \sigma_p(\widetilde{K}_D)$. In fact, let us assume $\phi \in L^2(D)$ is such that $\widetilde{K}_D[\phi] = 0$. Then from the definition of $\widetilde{K}_D$, we get that

$$0 = (\Delta + 1)\left(\widetilde{K}_D[\phi]\right) = \phi\,,$$

and therefore $\phi = 0$. This shows that $0 \notin \sigma_p(\widetilde{K}_D)$, and therefore our assertion for the operator $\widetilde{K}_D$ holds. A same argument applying to the operator $\widetilde{K}_D^*$ results in our second assertion that $\sigma(\widetilde{K}_D^*) \backslash \sigma_p(\widetilde{K}_D^*) = \{0\}$. □

Now, we are ready to apply Theorem 4.1 to $\widetilde{K}_D$ to obtain the following decomposition of the space $L^2(D)$.

Lemma 4.3. *Let the space E_λ be the generalized eigenspace of the operator $\widetilde{K}_D$ for the eigenvalue λ defined as in Theorem 4.1. Then the following decomposition holds*

$$L^2(D) = \overline{\bigoplus_{\lambda \in \sigma_p(\widetilde{K}_D)} E_\lambda}\,. \tag{4.1}$$

Proof. From Lemma 4.2, it follows directly that $0 \notin \sigma_p(\widetilde{K}_D^*)$ and $ker(\widetilde{K}_D^*) = \{0\}$. Hence we have that

$$L^2(D) = \Big(Ker(\widetilde{K}_D^*)\Big)^\perp = \overline{Ran(\widetilde{K}_D)}\,.$$

This proves the lemma after applying Theorem 4.1. □

We can now restrict the action of $\widetilde{K}_D$ on the invariant subspaces E_λ and consider the linear operator $(\widetilde{K}_D)\,|_{E_\lambda} \colon E_\lambda \to E_\lambda$ over the finite dimensional spaces E_λ. By directly applying the Jordan theory to the finite-dimensional linear operator $(\widetilde{K}_D)\,|_{E_\lambda}$, we get that E_λ can be decomposed into $E_\lambda = \bigoplus_{1 \le i \le N_\lambda} E_\lambda^i$ for some N_λ such the operator $(\widetilde{K}_D)\,|_{E_\lambda}$ can be written as

$$(\widetilde{K}_D)\,|_{E_\lambda} = \sum_{1 \le i \le N_\lambda} \widetilde{K}_{i,\lambda}, \tag{4.2}$$

where the operators $\widetilde{K}_{i,\lambda} : E_\lambda^i \to E_\lambda^i$ admit the action of the following Jordan block under a choice of basis $\mathbf{e}_\lambda^i$ in E_λ^i:

$$J_\lambda^i := \begin{pmatrix} \lambda & 1 & \dots & \dots & 0 \\ 0 & \lambda & 1 & \dots & 0 \\ \vdots & \vdots & \ddots & \vdots & \vdots \\ 0 & \dots & \dots & \lambda & 1 \\ 0 & \dots & \dots & \dots & \lambda \end{pmatrix}, \tag{4.3}$$

as matrices of size smaller than or equal to m_λ. With these notations at hand, we are now able to obtain a decomposition of the operator $\widetilde{K}_D$ by combining the decompositions of its respective restricted linear operators $(\widetilde{K}_D)\,|_{E_\lambda}$ as follows

$$\widetilde{K}_D = \sum_{\lambda \in \sigma_p(\widetilde{K}_D)} \sum_{1 \le i \le N_\lambda} \widetilde{K}_{i,\lambda}\,, \tag{4.4}$$

keeping in mind that a summation over λ stands for a direct sum over the respective actions in each invariant subspaces E_λ following the direct sum decomposition of $L^2(D)$ in (4.1). A similar argument for such a decomposition of the operator $\widetilde{K}_D$ can also be found in [26].

For the sake of simplicity, for a given $n \in \mathbb{N}$ and a given Riesz basis $\mathbf{w}$, i.e., a complete frame in $L^2(D)$, supposing that $\mathbf{v}$ is a finite subset of $\mathbf{w}$, we shall often write, for any $\phi \in L^2(D)$, $(\phi)_{\mathbf{v},L^2(D)} \in \mathbb{C}^n$ as the coefficients of ϕ in front of the vectors in $\mathbf{v}$ when expressed in the Riesz basis $\mathbf{w}$, i.e., if

$$\phi = \sum_{w_i \in \mathbf{w}} b_i w_i\,, \tag{4.5}$$

for coefficients $b_i \in \mathbb{C}$ and $\mathbf{v} = (w_{k_1}, w_{k_2}, \dots, w_{k_n})$, then $(\phi)_{\mathbf{v},L^2(D)} = (b_{k_1}, b_{k_2}, \dots, b_{k_n})$. Also, for any $a = (a_1, \dots, a_n) \in \mathbb{C}^n$, and any given finite frame $\mathbf{v} = (v_1, v_2, \dots, v_n)$ in $L^2(D)$, we write

$$\mathbf{v}^T a := \sum_{i=1}^n a_i v_i\,, \tag{4.6}$$

and, for any $\phi \in L^2(D)$, the L^2 inner product of $\mathbf{v}$ and ϕ as

$$\langle \mathbf{v}, \phi \rangle_{L^2(D)} := \left(\langle v_1, \phi \rangle_{L^2(D)}, \langle v_2, \phi \rangle_{L^2(D)}, \dots, \langle v_n, \phi \rangle_{L^2(D)} \right) \in \mathbb{C}^n \,. \tag{4.7}$$

With these notations, we can write (4.4) in terms of the frame $\bigcup_{\lambda \in \sigma_p(\tilde{K}_D)} \bigcup_{1 \le i \le N_\lambda} \mathbf{e}_\lambda$ as follows:

$$\widetilde{K}_D = \sum_{\lambda \in \sigma_p(\widetilde{K}_D)} \sum_{1 \le i \le N_\lambda} \left(\mathbf{e}_\lambda^i \right)^T J_\lambda^i (\,\cdot\,)_{\mathbf{e}_\lambda^i, L^2(D)}, \tag{4.8}$$

where the superscript T denotes the transpose as described in (4.6). Therefore, substituting the above expression of $\widetilde{K}_D$ into (2.19), we have

$$\begin{aligned} W_{nm}(D, \varepsilon^*) &= \left\langle J_n(r)e^{in\theta}, (\varepsilon^{*-1} + \tilde{K}_D)^{-1}[J_m(r)e^{im\theta}] \right\rangle_{L^2(D)} \\ &= \sum_{\lambda \in \sigma_p(\widetilde{K}_D)} \sum_{1 \le i \le N_\lambda} \left[\left\langle J_n(r)e^{in\theta}, \mathbf{e}_\lambda^i \right\rangle_{L^2(D)} \right]^T [J^i_{\varepsilon^{*-1}+\lambda}]^{-1} \left[J_m(r)e^{im\theta} \right]_{\mathbf{e}_\lambda^i, L^2(D)} . \end{aligned} \tag{4.9}$$

The above expression gives a general decomposition of the scattering coefficient $W_{nm}(D, \varepsilon^*)$.

Next, we consider the special domain $D = B(0, R)$. From Proposition 2.7 we shall focus on the operators $\widetilde{K}_m^{(1)}$ for $m \in \mathbb{Z}$. Similar to the previous argument, we can see that the operators $\widetilde{K}_m^{(1)}$ are compact on $L^2((0, R), r\,dr)$. Moreover, it is direct to obtain the following lemma for $\widetilde{K}_m^{(1)}$ similar to Lemma 4.2.

Lemma 4.4. *Let $\widetilde{K}_m^{(1)}$ be defined as in (2.29), and $\left(\widetilde{K}_m^{(1)}\right)^*$ be its L^2 adjoint, then we have*

$$\sigma(\widetilde{K}_m^{(1)}) \backslash \sigma_p(\widetilde{K}_m^{(1)}) = \{0\} \quad \text{and } \sigma\left(\left(\widetilde{K}_m^{(1)}\right)^*\right) \backslash \sigma_p\left(\left(\widetilde{K}_m^{(1)}\right)^*\right) = \{0\} \,.$$

Proof. We follow a same argument as in the proof of Lemma 4.2. By directly applying Theorem 4.1, it suffices to show that $0 \notin \sigma_p(\widetilde{K}_m^{(1)})$, in order to prove our claim for $\widetilde{K}_m^{(1)}$. Assume $\phi \in L^2((0, R), r\,dr)$ is such that $\widetilde{K}_m^{(1)}[\phi] = 0$. Then from the definition of $\widetilde{K}_m^{(1)}$, we get that

$$0 = \left(\frac{1}{r}\partial_r r \partial_r + 1 - \frac{m^2}{r^2} \right) \left(\tilde{K}_m^{(1)} \phi(r) \right) e^{im\theta} = (\Delta + 1)\tilde{K}^{(1)} \left(\phi(r) e^{im\theta} \right) = \phi(r) e^{im\theta} \,,$$

which gives $\phi = 0$. This proves our assertion for the operator $\widetilde{K}_m^{(1)}$. The same argument applies to $\left(\widetilde{K}_m^{(1)}\right)^*$ for the remaining part of our assertion. □

A same argument as in the proof of Lemma 4.3 results in the following lemma.

Lemma 4.5. *Let the space $E_{m,\lambda}$ be the generalized eigenspace of the operator $\widetilde{K}_m^{(1)}$ for the eigenvalue λ defined as in Theorem 4.1. Then the following decomposition holds*

$$L^2((0, R), r\,dr) = \overline{\bigoplus_{\lambda \in \sigma_p\left(\widetilde{K}_m^{(1)}\right)} E_{m,\lambda}} \,. \tag{4.10}$$

Following a same argument as we did for $\widetilde{K}_D$ to the new operator $\widetilde{K}_m$, we apply the Jordan decomposition theorem to the finite-dimensional linear operator $(\widetilde{K}_m) \,|_{E_{m,\lambda}} \colon E_{m,\lambda} \to E_{m,\lambda}$ over the invariant subspace. Combining this with the previous lemma, we get that there exists a complete basis $\bigcup_\lambda \bigcup_{0 \le i \le N_\lambda^m} \mathbf{e}_{m,\lambda}^i$ over $L^2((0, R), r\,dr)$ with each $\mathbf{e}_{m,\lambda}^i$ spanning the subspace $E_{m,\lambda}^i$ such that $\widetilde{K}_m$ admits

the action of a Jordan block, denoted by $J^i_{m,\lambda}$, with respect to the basis when acting on the invariant subspace $E^i_{m,\lambda}$. Moreover, adopting the same notations as previously introduced, we can write

$$\left(\varepsilon^{*-1} + \tilde{K}_m^{(1)}\right)^{-1} = \sum_{\lambda \in \sigma_p(\widetilde{K}_m^{(1)})} \sum_{1 \le i \le N_\lambda^m} \left(\mathbf{e}^i_{m,\lambda}\right)^T [J^i_{m,\varepsilon^{*-1}+\lambda}]^{-1} (\,\cdot\,)_{\mathbf{e}^i_{m,\lambda}, L^2((0,R),r\,dr)}, \tag{4.11}$$

and a similar expansion holds for $\tilde{K}_m^{(2)}$. Again, we keep in mind that the summation over λ stands for a direct sum over the respective actions in each invariant subspaces $E_{m,\lambda}$ following the direct sum decomposition of $L^2((0,R),r\,dr)$ in (4.10).

Now, using the orthogonality of $\{e^{im\theta}\}_{m\in\mathbb{Z}}$ on $L^2(\mathbb{S}^1)$, for a given contrast ε^* such that $-\varepsilon^{*-1}$ is not an eigenvalue of $\tilde{K}_m^{(1)}$, we have that

$$\begin{aligned} & W_{nm}(D,\varepsilon^*) \\ = \;& \delta_{nm} \left\langle J_n, \left(\varepsilon^{*-1} + \tilde{K}_m^{(1)}\right)^{-1} [J_m] \right\rangle_{L^2((0,R),r\,dr)} \\ = \;& \delta_{nm} \sum_{\lambda \in \sigma(\widetilde{K}_m^{(1)})} \sum_{1 \le i \le N_\lambda^m} [\langle J_n(r), \mathbf{e}^i_{m,\lambda}\rangle_{L^2((0,R),rdr)}]^T [J^i_{m,\varepsilon^{*-1}+\lambda}]^{-1} (\, J_m(r)\,)_{\mathbf{e}^i_{m,\lambda}, L^2((0,R),r\,dr)}. \end{aligned} \tag{4.12}$$

Finally, the following remarks are in order. For $D = B(0,R)$, the action of $\tilde{K}_D$ on each of the subspace $E^i_{m,\lambda} e^{im\theta}$ of $L^2(D)$ is invariant and admits the same Jordan block representation as $\widetilde{K}_m^{(1)}$ acting on $E^i_{m,\lambda}$ of $L^2((0,R),rdr)$. Hence, the decomposition

$$L^2(D) = \overline{\bigoplus_{m\in\mathbb{Z}} \bigoplus_{\lambda \in \sigma_p\left(\widetilde{K}_m^{(1)}\right)} \bigoplus_{1 \le i \le N_\lambda^m} E^i_{m,\lambda} e^{im\theta}}$$

coincides with the original Jordan block decomposition of $\tilde{K}_D$,

$$L^2(D) = \overline{\bigoplus_{\lambda_p \in \sigma(\widetilde{K})} \bigoplus_{1 \le i \le N_\lambda} E^i_\lambda}\,.$$

Therefore, we readily get $\bigcup_{m\in\mathbb{Z}} \sigma_p(\widetilde{K}_m^{(1)}) = \sigma_p(\tilde{K}_D)$, and the sum (4.12) constitutes a part of the sum (4.9) with all the other terms in (4.9) being zero. In the next section, we will focus on the decay of the eigenvalues of $\tilde{K}_m$ and the asymptotic expansion for the eigenvalues and eigenfunctions of the operators. This will allow us to better understand the behavior of W_{nm} and $C(\varepsilon^*, n, m)$.

4.2. Asymptotics of the eigenvalues and eigenfunctions of $\widetilde{K}_m^{(i)}$

Intuitively, we can expect that the eigenvalues of $\widetilde{K}_m^{(1)}$ are distributed closer to 0 as $|m|$ increases for the following reason. Considering (2.33) together with the asymptotic expressions (2.27) and (2.35) of J_m and Y_m as $m \to \infty$, we have the following bound for the operator norm of $\tilde{K}_m$ for $m \in \mathbb{Z}$:

$$||\widetilde{K}_m^{(1)}||_{L^2((0,R)rdr)} \le \frac{C'_R}{m^2} \tag{4.13}$$

for some constant C'_R depending on R. Then we obtain the estimate for the spectral radius of $\tilde{K}_m$ from the Gelfand theorem:

$$\sup_{\lambda \in \sigma(\widetilde{K}_m^{(1)})} |\lambda| = \lim_{n\to\infty} \left|\left| \left(\widetilde{K}_m^{(1)}\right)^n \right|\right|^{\frac{1}{n}} \le \frac{C'_R}{m^2}. \tag{4.14}$$

This implies that the spectrum $\sigma(\widetilde{K}_m^{(1)})$ actually lies inside $\sigma(\tilde{K})\bigcap B(0,\frac{C'_R}{m^2})$. However, this argument is heuristic.

Therefore, we intend to obtain a rigourous asymptotic expansion of the eigenvalues for the operators $\tilde{K}_m$. For this purpose, we first restrict ourselves to the discussion of the operators for $m\in\mathbb{N}$, and consider the equation $\tilde{K}_m^{(1)}f=\lambda f$ with $\lambda\neq 0$. Since we have

$$\left(\frac{1}{r}\partial_r r\partial_r+1-\frac{m^2}{r^2}\right)\left(\tilde{K}_m^{(1)}f\right)e^{im\theta}=(\Delta+1)\tilde{K}^{(1)}\left(fe^{im\theta}\right)=fe^{im\theta}, \tag{4.15}$$

we obtain for $m\neq 0$ the following equivalence

$$\tilde{K}_m^{(1)}f=\lambda f \quad\Leftrightarrow\begin{cases}\left(\frac{1}{r}\partial_r r\partial_r+1-\frac{1}{\lambda}-\frac{m^2}{r^2}\right)f & =0\,,\\ f(0) & =0\,,\\ f(R) & =-\frac{i}{4}\int_0^R rJ_m(r)f(r)drH_m^{(i)}(R)\,.\end{cases} \tag{4.16}$$

Enumerating the eigenvalues λ of $\tilde{K}_m^{(1)}$ as $\lambda_{m,l}$ in descending order of their magnitudes, and writing $e^i_{m,l}$ as the unique eigenfunction in the Jordan basis $\mathbf{e}^i_{m,\lambda_{m,l}}$ for each i, we are bound to have the following form for the eigenpair of the operator for all i,

$$(\lambda_{m,l},e^i_{m,l})=\left(\lambda_{m,l},J_m\left(\sqrt{1-\frac{1}{\lambda_{m,l}}}r\right)\right)\,. \tag{4.17}$$

The above statement implies that the geometric multiplicities of all the eigenvalues of $\tilde{K}_m^{(1)}$ should be $N_\lambda=1$ (while the algebraic multiplicities are still unknown for the time being). For the sake of simplicity, we denote the frame $\mathbf{e}^1_{m,\lambda_{m,l}}$ by $\mathbf{e}_{m,l}$, and also the eigenfunction $e^1_{m,l}$ by $e_{m,l}$. Substituting (4.17) into (4.16), together with the following well-known property of Lommel's integrals [24] that for all $n\in\mathbb{N}$ and for all $a,b>0$ with $a\neq b$:

$$\int_0^R[J_n(ar)]^2rdr = \frac{R^2}{2}[J_n(aR)^2-J_{n-1}(aR)J_{n+1}(aR)]\,, \tag{4.18}$$

$$\int_0^R J_n(ar)J_n(br)rdr = \frac{R}{a^2-b^2}[bJ_n(aR)J_{n-1}(bR)-aJ_{n-1}(aR)J_n(bR)]\,, \tag{4.19}$$

we get the following equation for $\lambda_{m,l}$:

$$\begin{aligned}&J_m\left(\sqrt{1-\frac{1}{\lambda_{m,l}}}R\right)\\ =\;&\frac{i}{4}R\lambda_{m,l}H_m^{(i)}(R)\left[\sqrt{1-\frac{1}{\lambda_{m,l}}}J_m(R)J_{m-1}\left(\sqrt{1-\frac{1}{\lambda_{m,l}}}R\right)\right.\\ &\left.-J_{m-1}(R)J_m\left(\sqrt{1-\frac{1}{\lambda_{m,l}}}R\right)\right]\,.\end{aligned} \tag{4.20}$$

Now since $\lambda_{m,l}\to 0$ as $l\to\infty$, from the following well-known asymptotic of J_n [24] for all n:

$$J_n(z)=\sqrt{\frac{2}{\pi z}}\cos\left(z-\frac{2n+1}{4}\pi\right)+O(z^{-3/2})\,, \tag{4.21}$$

we obtain the following estimate for $m,n,l\in\mathbb{N}$:

$$J_n\left(\sqrt{1-\frac{1}{\lambda_{m,l}}}R\right)=\sqrt{\frac{2}{\pi R\sqrt{1-\frac{1}{\lambda_{m,l}}}}}\cos\left(\sqrt{1-\frac{1}{\lambda_{m,l}}}R-\frac{2n+1}{4}\pi\right)+O(|\lambda_{m,l}|^{3/4})\,. \tag{4.22}$$

Hence, substituting this expression into (4.20), we shall directly infer that the eigenvalues $\lambda_{m,l}$ satisfy the following bound:

$$J_m\left(\sqrt{1-\frac{1}{\lambda_{m,l}}}R\right) = O(|\lambda_{m,l}|^{3/4})\,, \tag{4.23}$$

which has a decay order higher than the one in (4.22). With this observation, we shall expect that the terms $\sqrt{1-\frac{1}{\lambda_{m,l}}}R$ should be close to the l-th zeros of the Bessel functions of J_m as l grows, which is indeed the case following the argument below.

For the sake of exposition, we shall often denote by $a_{m,l}$ the zeros of the m-th Bessel function of the first kind, i.e., $J_m(a_{m,l}) = 0$, arranged in ascending order. Then it follows from (4.21), the inverse function theorem and the Taylor expansion that

$$\left|a_{m,l} - \frac{2m+4l-1}{4}\pi\right| < C(m+2l)^{-1/2} \to 0 \quad \text{as } l \to \infty\,. \tag{4.24}$$

Then, again from (4.21), we have

$$J_m'\left(a_{m,l}\right) - (-1)^l\sqrt{\frac{2}{\pi a_{m,l}}} = O({a_{m,l}}^{-3/2})\,, \tag{4.25}$$

which, combined with (4.23), leads to

$$R\sqrt{1-\frac{1}{\lambda_{m,l}}} - a_{m,l} = O({a_{m,l}}^{-1/2})\,. \tag{4.26}$$

This gives us the following estimate for $\lambda_{m,l}$:

$$R\sqrt{1-\frac{1}{\lambda_{m,l}}}\Big/\left(\frac{(m+2l)\pi}{2} - \frac{\pi}{4}\right) \to 1 \quad \text{as } l \to \infty\,. \tag{4.27}$$

Therefore, we obtain the following decay rate of the eigenvalues,

$$\lambda_{m,l}\Big/\left(\frac{4R^2}{\pi^2}\frac{1}{(m+2l)^2}\right) \to -1 \quad \text{as } l \to \infty\,. \tag{4.28}$$

Moreover, using (4.26) and the fact that J_m is holomorphic, we have the following uniform estimate for the eigenfunctions:

$$\left|\left|J_m\left(\sqrt{1-\frac{1}{\lambda_{m,l}}}r\right) - J_m\left(\frac{a_{m,l}}{R}r\right)\right|\right|_{\mathcal{C}^0((0,R))} \le C||J_m'||_{L^\infty((0,R))}{a_{m,l}}^{-1/2} < C(m+2l)^{-1/2}\,. \tag{4.29}$$

Note that the set $\{J_m\left(\frac{a_{m,l}}{R}r\right)\}_{l=1}^\infty$ forms a complete orthogonal basis in $L^2((0,R),\, r\,dr)$. Hence, the above estimate actually implies that the eigenfunctions of $\tilde{K}_m^{(1)}$ approach in the sup-norm to an orthogonal basis in $L^2((0,R),\, r\,dr)$ for all $m \in \mathbb{N}$. From (2.33), together with the fact that $a_{-m,l} = a_{m,l}$ from (2.32), the above analysis also holds for $\tilde{K}_{-m}^{(1)}$.

The following theorem summarizes the main eigenvalue and eigenfunction estimates for the operator $\tilde{K}_m^{(1)}$.

Theorem 4.6. *For all $m \in \mathbb{Z}\backslash\{0\}$, the eigenpairs of the operator $\tilde{K}_m^{(1)}$ are of the form*

$$(\lambda_{m,l}, e_{m,l}) = \left(\lambda_{m,l}, J_m\left(\sqrt{1-\frac{1}{\lambda_{m,l}}}r\right)\right) \quad \textit{for } l \in \mathbb{N}\,, \tag{4.30}$$

where the eigenvalues $\lambda_{m,l}$ satisfy the following asymptotic behavior

$$\lambda_{m,l} \Big/ \left(\frac{4R^2}{\pi^2} \frac{1}{(|m|+2l)^2} \right) \to -1 \quad \text{as } l \to \infty \,. \tag{4.31}$$

Moreover, the eigenfunctions also have the following uniform estimate:

$$\left\| J_m\left(\sqrt{1 - \frac{1}{\lambda_{m,l}}} r \right) - J_m\left(\frac{a_{m,l}}{R} r \right) \right\|_{\mathcal{C}^0((0,R))} = O((|m|+2l)^{-1/2}) \,. \tag{4.32}$$

This theorem is very important for the analysis of the behaviors of W_{nm} and $C(\varepsilon^*, n, m)$. Figure 1 shows the distribution of eigenvalues of $\tilde{K}_m^{(1)}$ for $R = 10$ with different values of m. It not only illustrates that the spectral radius decreases as the value of m increases (which agrees with the estimate (4.14)); but also that, for a fixed number $l \in \mathbb{N}$, the magnitude of the l-th eigenvalue of $\tilde{K}_m^{(1)}$ decreases in general monotonically with respect to increment of m (which agrees with (4.31)). Eigenfunctions of $\tilde{K}_m^{(1)}$ for some values of m are also plotted in Figure 2 for a better illustration of the behaviour of eigenfunctions.

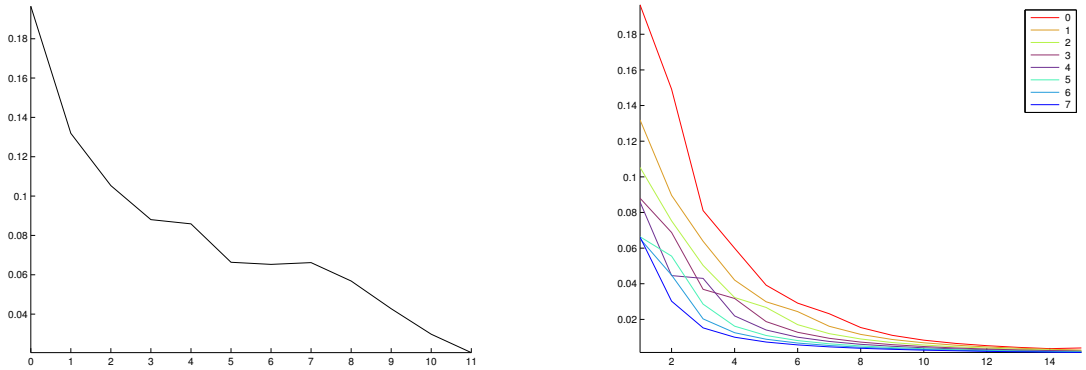

(a) (b)

Figure 1: (a) Spectral radius of $\tilde{K}_m^{(1)}$ for $m = 0, 1, \ldots, 11$. (b) Norms of eigenvalues $\lambda_{m,l}, l = 1, 2, \ldots, 15$, for operators $\tilde{K}_m^{(1)}, m = 0, 1, \ldots, 7$, as in the legend.

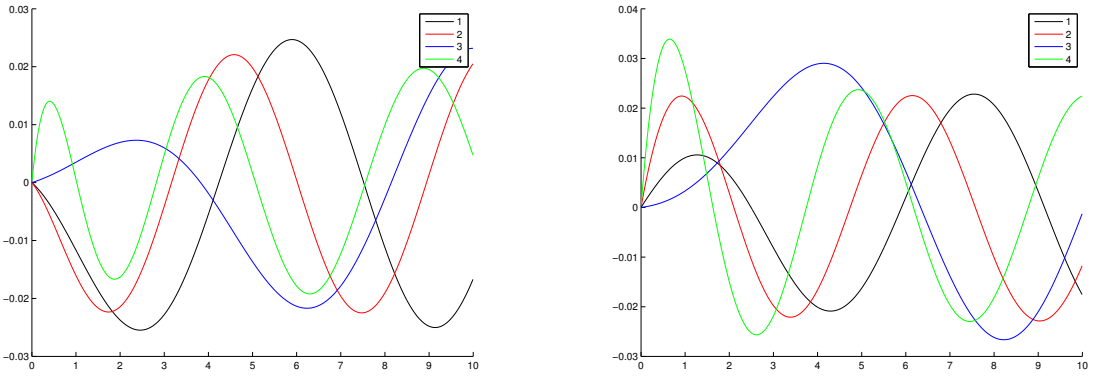

(1a) (1b)

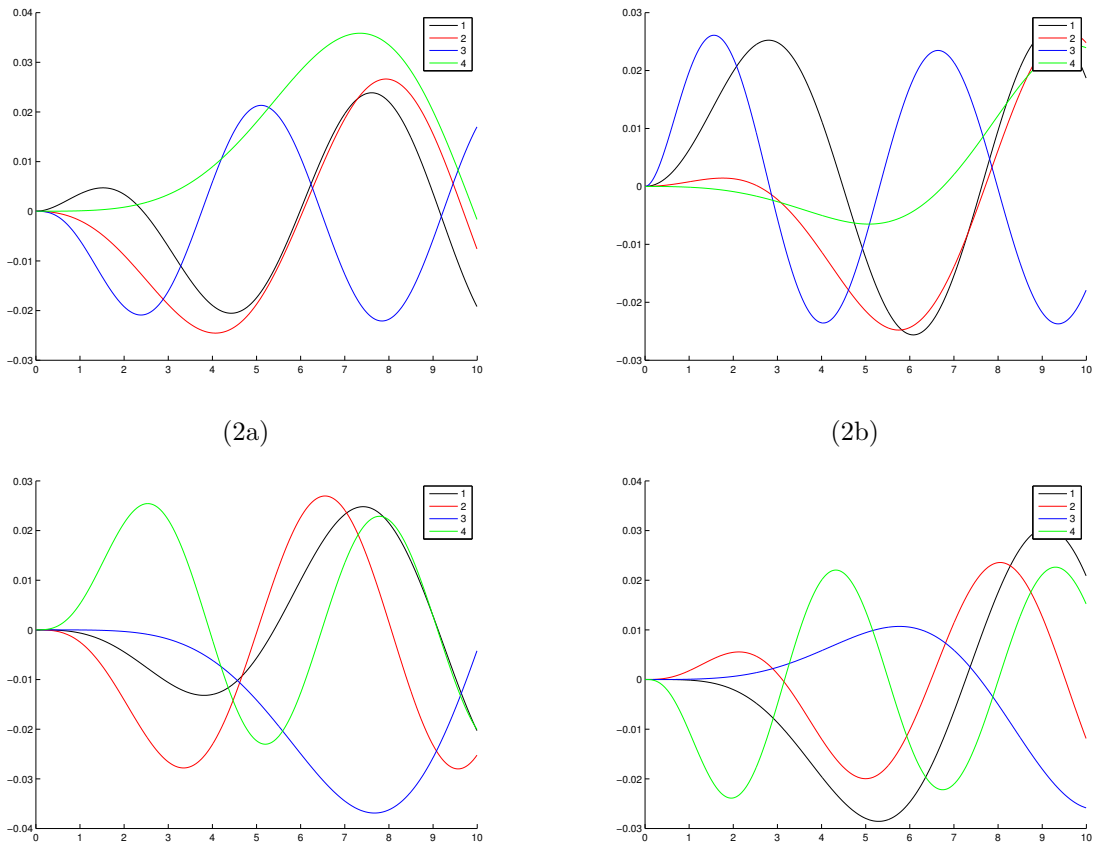

Figure 2: Real and imaginary parts of the first 4 eigenfunctions of $\tilde{K}_m^{(1)}$, $m = 1, 2, 3$. (1a) Real parts of eigenfunctions of $\tilde{K}_1^{(1)}$; (1b) imaginary parts of eigenfunctions of $\tilde{K}_1^{(1)}$; (2a) real parts of eigenfunctions of $\tilde{K}_2^{(1)}$, and so forth.

4.3. Tail behavior of the series representation of W_{nm} and $C(\varepsilon^*, n, m)$ and the super-resolution phenomenon

In this subsection, we deduce very useful information on the behaviors of W_{nm} and $C(\varepsilon^*, n, m)$ from the asymptotic behaviors of eigenpairs of $\tilde{K}_m^{(1)}$ derived in the previous subsection.

4.3.1. Tail behavior of the series representation of W_{nm}

We first focus on the scattering coefficients $W_{nm}(D, \varepsilon^*)$ when $D = B(0, R)$. Form (2.34), it is known that $W_{nm} = 0$ when $n \neq m$, therefore the only interesting case is when $n = m$. Again, we shall first consider $m \in \mathbb{N}$. From the analysis in the previous subsection that the geometric multiplicities of all the eigenvalues of $\tilde{K}_m^{(1)}$ are $N_\lambda^m = 1$, we already obtain from (4.12) that

$$W_{mm}(D, \varepsilon^*) = \sum_{l=0}^{\infty} [\langle J_m(r), \mathbf{e}_{m,l} \rangle_{L^2((0,R), r dr)}]^T [J_{m, \varepsilon^{*-1} + \lambda_{m,l}}]^{-1} (\, J_m(r)\,)_{\mathbf{e}_{m,l}, L^2((0,R), r\, dr)}.$$

For the sake of simplicity, from now on we shall often denote

$$\widetilde{\lambda_{m,l}} := \frac{1}{1 - \frac{a_{m,l}^2}{R^2}} \quad \text{and} \quad \widetilde{e_{m,l}} := J_m\left(\frac{a_{m,l}}{R} r\right). \tag{4.33}$$

From (4.18) and (4.32), together with the completeness and orthogonality of $\widetilde{e_{m,l}}$ in $L^2((0,R),\, r\,dr)$ and the Parseval's identity, we readily obtain that, fixing any $m \in \mathbb{N}$ and for any given ϵ, there exists $N(m)$ such that for all $i > N(m)$, we have

$$\left| \langle e_{m,i}, \widetilde{e_{m,j}} \rangle_{L^2((0,R),rdr)} - \delta_{ij} \frac{R^2}{2} J_{m+1}^2(a_{m,j}) \right| < \epsilon_{ij}\,, \tag{4.34}$$

where $\sum_j \epsilon_{ij}^2 < \epsilon^2$. Therefore, for a large $N_1(m)$, the span of $\{e_{m,l}\}_{l=N_1(m)}^{\infty}$ has a finite dimensional orthogonal complement. This follows that there exists a large $N_2(m) > N_1(m)$ such that the algebraic multiplicity of $\lambda_{m,l}$ is 1. Therefore, we directly obtain

$$W_{mm}(D, \varepsilon^*) \quad = \quad S_{1,m}(\varepsilon^*) + S_{2,m}(\varepsilon^*), \tag{4.35}$$

where the sums $S_{i,m}(\varepsilon^*)$, $i = 1, 2$, are defined by

$$S_{1,m}(\varepsilon^*) \quad := \quad \sum_{l=0}^{N_2(m)} [\langle J_m(r), \mathbf{e}_{m,l} \rangle_{L^2((0,R),rdr)}]^T [J_{m,\varepsilon^{*-1}+\lambda_{m,l}}]^{-1} (\, J_m(r)\,)_{\mathbf{e}_{m,l}, L^2((0,R),r\,dr)} \tag{4.36}$$

$$S_{2,m}(\varepsilon^*) \quad := \quad \sum_{l=N_2(m)+1}^{\infty} \frac{\alpha_{m,l}}{\varepsilon^{*-1} + \lambda_{m,l}}\,, \tag{4.37}$$

with the coefficients $\alpha_{m,l}$ being defined, for all m, l, as

$$\alpha_{m,l} := \langle J_m(r), e_{m,l} \rangle_{L^2((0,R),rdr)} (\, J_m(r)\,)_{e_{m,l}, L^2((0,R),r\,dr)}. \tag{4.38}$$

Note that for any $\varepsilon^* \geq -2\,\mathrm{Re}\left(\lambda_{m,N_2(m)}^{-1}\right)$, we have $|S_{1,m}(\varepsilon^*)| < C_m$ for some constant C_m. Therefore, if we want to investigate the behavior of (4.35) for large ε^*, we shall focus on the term $S_{2,m}(\varepsilon^*)$. For this purpose, we analyze the limiting behavior of $\alpha_{m,l}$ as l increases. Now, from (4.19) and (4.32), we have the following estimate for the inner product:

$$\langle J_m(r), e_{m,l} \rangle_{L^2((0,R),rdr)} - \widetilde{\lambda_{ml}} a_{m,l} J_m(R) J_{m-1}(a_{m,l}) = O(a_{m,l}^{-1/2})\,. \tag{4.39}$$

From (4.21) we get

$$J_{m\pm1}\,(a_{m,l}) - (-1)^l \sqrt{\frac{2}{\pi a_{m,l}}} = O({a_{m,l}}^{-3/2})\,, \tag{4.40}$$

and hence it follows that

$$\langle J_m(r), e_{m,l} \rangle_{L^2((0,R),rdr)} \Big/ (-1)^l \widetilde{\lambda_{m,l}} a_{m,l}^{1/2} \sqrt{\frac{2}{\pi}} J_m(R) \to 1 \quad \text{ as } l \to \infty\,. \tag{4.41}$$

From (4.34), we obtain that the coefficient of $J_m(r)$ of $e_{m,l}$ with respect to the Jordan basis approaches to the orthogonal project of $J_m(r)$ on the subspace $e_{m,l}$, whence the following holds

$$(\, J_m(r)\,)_{e_{m,l}, L^2((0,R),r\,dr)} \Big/ \frac{\langle J_m(r), e_{m,l} \rangle_{L^2((0,R),rdr)}}{\frac{R^2}{2}[J_{m-1}^2(a_{m,l})]} \to 1 \quad \text{ as } l \to \infty\,. \tag{4.42}$$

Combining the above several limiting behaviors (4.41) and (4.42) yields

$$\alpha_{m,l} \Big/ 2\widetilde{\lambda_{m,l}}^{\,2} a_{m,l}^2 \frac{J_m^2(R)}{R^2} \to 1 \quad \text{ as } l \to \infty\,, \tag{4.43}$$

which can further be reduced to the following asymptotic behavior by combining (4.26),(4.28) and (4.33),

$$\alpha_{m,l} \Big/ 2\lambda_{m,l} J_m^2(R) \to -1 \quad \text{ as } l \to \infty\,. \tag{4.44}$$

From (2.32) and (2.33), the conclusions also hold for the case with $-m \in \mathbb{N}$.

The above analysis can be summarized in the following theorem.

Theorem 4.7. *Let $D = B(0,R)$ be a circular domain. For all $m \in \mathbb{Z}\backslash\{0\}$, there exist constants $N(m) \in \mathbb{N}$ and $C_m > 0$ such that, for any given contrast value $\varepsilon^* > -2\,Re\left(\lambda_{m,N(m)}^{-1}\right)$, the scattering coefficient $W_{mm}(D,\varepsilon^*)$ has the following decomposition*

$$W_{mm}(D,\varepsilon^*) \quad = \quad S_{1,m}(\varepsilon^*) + S_{2,m}(\varepsilon^*), \tag{4.45}$$

where $S_{1,m}(\varepsilon^*)$ has a uniform bound

$$|S_{1,m}(\varepsilon^*)| < C_m\,, \tag{4.46}$$

whereas $S_{2,m}(\varepsilon^*)$ is of the form

$$S_{2,m}(\varepsilon^*) = \sum_{l=N_2(m)+1}^{\infty} \frac{\alpha_{m,l}}{\varepsilon^{*-1} + \lambda_{m,l}}, \tag{4.47}$$

where the coefficients $\alpha_{m,l}$ have the following limiting behavior

$$\alpha_{m,l} \Big/ 2\lambda_{m,l} J_m^2(R) \to -1 \quad \text{ as } l \to \infty\,. \tag{4.48}$$

This decomposition of the coefficient W_{mm} gives us a clear picture of the behavior of W_{mm} as ε^* grows. When ε^* increases, ε^{*-1} passes through the values $-\mathrm{Re}(\lambda_{m,l}) \sim (|m|+2l)^{-2}$ for large l. If $\lambda_{m,l} \in \mathbb{R}$, ε^{*-1} directly passes through the pole. Therefore W_{mm} grows from a finite value rapidly to a directional complex infinity $\infty e^{i\theta}$ for some θ, and then comes back from $-\infty e^{i\theta}$ to a finite value after ε^{*-1} passes through it. Otherwise, if $\lambda_{m,l} \notin \mathbb{R}$, then ε^{*-1} does not directly hit the pole. However, since $\lambda_{m,l} \sim -(|m|+2l)^{-2}$ where $(|m|+2l)^{-2}$ are real, $\mathrm{Im}(\lambda_{m,l})$ is very small for large l. Hence, as ε^{*-1} moves close to $-\mathrm{Re}(\lambda_{m,l})$, it comes close to the pole. Therefore, W_{mm} grows from a comparably small value very rapidly to a complex value of very large modulus, and then drops back to a small value after passing through $-\mathrm{Re}(\lambda_{m,l})$. The behavior of W_{mm} is consequently very oscillatory as ε^* grows. Moreover, from (4.48) we have for a fixed pair of m,l that

$$\frac{\alpha_{m,l}}{\varepsilon^{*-1} + \lambda_{m,l}} \to -2J_m^2(R) \tag{4.49}$$

as $\varepsilon^* \to \infty$, and therefore it is clear that there is no hope on any convergence behavior of W_{mm} as ε^* grows to infinity.

Furthermore, from (4.31) that the asymptotic $\lambda_{m,l} \sim -(|m|+2l)^{-2}$ holds and the limit comparison test, we have for a fixed $\varepsilon^* > -2\,\mathrm{Re}\left(\lambda_{m,N(m)}^{-1}\right)$ that

$$|W_{nm}(D,\varepsilon^*)| \quad \leq \quad \delta_{nm}\left(C_m + \frac{C'_m}{d(-\varepsilon^{*-1}, \sigma(\tilde{K}_m^{(1)}))} J_m^2(R) \sum_{l=0}^{\infty} |\lambda_{m,l}|\right) \tag{4.50}$$

$$\leq \quad \delta_{nm}\left(C_m + \frac{C'_m}{d(-\varepsilon^{*-1}, \sigma(\tilde{K}_m^{(1)}))} \frac{R^{|m|+|n|}}{|m|^{|m|}|n|^{|n|}}\right). \tag{4.51}$$

Corollary 4.8. *Let $D = B(0,R)$. For all $m \in \mathbb{Z}\backslash\{0\}$, there exist constants $N(m) \in \mathbb{N}$ and $C_{i,m}$, $i = 1,2$ such that, for any given contrast value $\varepsilon^* > -2\,Re\left(\lambda_{m,N(m)}^{-1}\right)$, the scattering coefficient $W_{nm}(D,\varepsilon^*)$ satisfies the following estimate for all $n \in \mathbb{Z}$,*

$$|W_{nm}(D,\varepsilon^*)| \leq \delta_{nm}\left(C_{1,m} + \frac{C_{2,m}}{d(-\varepsilon^{*-1}, \sigma(\tilde{K}_m^{(1)}))} \frac{R^{|m|+|n|}}{|m|^{|m|}|n|^{|n|}}\right). \tag{4.52}$$

This clearly improves the estimate (2.37).

4.3.2. Tail behavior of the series representation of $C(\varepsilon^*, n, m)$

We now focus on the behaviors of the coefficients $C(\varepsilon^*, n, m)$, which will help us to understand the phenomenon of super-resolution. We first focus on the case when $n, m \in \mathbb{N}$. We recall the expression of the coefficient $C(\varepsilon^*, n, m)$ in (3.27):

$$C(\varepsilon^*, n, m) := \varepsilon^{*-1} \left[\left(\varepsilon^{*-1} + \tilde{K}_m^{(1)} \right)^{-1} [J_m] \right] (R) \left[\left(\varepsilon^{*-1} + \tilde{K}_n^{(1)} \right)^{-1} [J_n] \right] (R) .$$

It remains to study the term $\left(\varepsilon^{*-1} + \tilde{K}_m^{(1)} \right)^{-1} [J_m](R)$. From the previous subsection, the geometric multiplicities of all the eigenvalues of $\tilde{K}_m^{(1)}$ are $N_\lambda^m = 1$, and the algebraic multiplicities of eigenvalues $\lambda_{m,l}$ of $\tilde{K}_m^{(1)}$ are also 1 for $l > N_2(m)$ (see Theorem 4.7). Together with the regularity of J_m, we readily obtain as in the previous subsection that

$$C(\varepsilon^*, n, m) = \varepsilon^{*-1}(s_{1,n}(\varepsilon^*) + s_{2,n}(\varepsilon^*))(s_{1,m}(\varepsilon^*) + s_{2,m}(\varepsilon^*)), \tag{4.53}$$

where the sums $s_{i,m}(\varepsilon^*)$, $(i = 1, 2)$ are defined by

$$s_{1,m}(\varepsilon^*) := \sum_{l=0}^{N_2(m)} (\mathbf{e}_{m,l}(R))^T [J_{m,\varepsilon^{*-1}+\lambda_{m,l}}]^{-1} (\, J_m(r)\,)_{\mathbf{e}_{m,l}, L^2((0,R), r\,dr)}, \tag{4.54}$$

$$s_{2,m}(\varepsilon^*) := \sum_{l=N_2(m)+1}^{\infty} \frac{\beta_{m,l}}{\varepsilon^{*-1} + \lambda_{m,l}} \tag{4.55}$$

with the coefficients $\beta_{m,l}$ being given for all m, l by

$$\beta_{m,l} := (\, J_m(r)\,)_{e_{m,l}, L^2((0,R), r\,dr)} J_m \left(\sqrt{1 - \frac{1}{\lambda_{m,l}}} R \right). \tag{4.56}$$

Similarly to the previous subsection, for any $\varepsilon^* \geq -2 \operatorname{Re} \left(\lambda_{m,N_2(m)}^{-1} \right)$, we have $|s_{1,m}(\varepsilon^*)| < C_m$ for some constant C_m. Therefore, we can study the behavior of (4.53) for large ε^* by investigating the limiting behavior of $\beta_{m,l}$ in the series $s_{2,m}(\varepsilon^*)$.

Substituting (4.22), (4.26) and (4.28) into (4.20), we readily derive

$$J_m \left(\sqrt{1 - \frac{1}{\lambda_{m,l}}} R \right) \Big/ (-1)^l \frac{i}{4} \lambda_{m,l} a_{m,l}^{1/2} H_m^{(1)}(R) J_m(R) \sqrt{\frac{2R}{\pi}} \to 1 \quad \text{as } l \to \infty . \tag{4.57}$$

Together with (4.41) and (4.42), we conclude that

$$\beta_{m,l} \Big/ \frac{i}{2} \sqrt{R} \lambda_{m,l} J_m^2(R) H_m^{(1)}(R) \to -1 \quad \text{as } l \to \infty . \tag{4.58}$$

Combining the above results with (2.32) and (2.33), we obtain the following decomposition of $C(\varepsilon^*, n, m)$.

Theorem 4.9. *Let $D = B(0, R)$ be a circular domain. For all $p \in \mathbb{Z}\backslash\{0\}$, there exist constants $N(p) \in \mathbb{N}$ and $C_p > 0$ such that, for any $n, m \in \mathbb{Z}\backslash\{0\}$ and any contrast value $\varepsilon^* > -2 \max \left\{ Re \left(\lambda_{n,N(n)}^{-1} \right), Re \left(\lambda_{m,N(m)}^{-1} \right) \right\}$, the coefficient $C(\varepsilon^*, n, m)$ (3.27) admits the following decomposition:*

$$C(\varepsilon^*, n, m) = \varepsilon^{*-1}(s_{1,n}(\varepsilon^*) + s_{2,n}(\varepsilon^*))(s_{1,m}(\varepsilon^*) + s_{2,m}(\varepsilon^*)) . \tag{4.59}$$

For all $p \in \mathbb{Z}\backslash\{0\}$, $s_{1,p}(\varepsilon^*)$ satisfies the uniform bound

$$|s_{1,p}(\varepsilon^*)| < C_p , \tag{4.60}$$

whereas $s_{2,p}(\varepsilon^*)$ is given by

$$s_{2,p}(\varepsilon^*) = \sum_{l=N_2(p)+1}^{\infty} \frac{\beta_{p,l}}{\varepsilon^{*-1} + \lambda_{p,l}}, \tag{4.61}$$

where the coefficients $\beta_{p,l}$ have the following limiting behavior

$$\beta_{p,l} \Big/ \frac{i}{2}\sqrt{R}\lambda_{p,l} J_p^2(R) H_p^{(1)}(R) \to -1 \quad \text{as } l \to \infty\,. \tag{4.62}$$

Similarly to the previous subsection, the aforementioned decomposition of $C(\varepsilon^*, n, m)$ clearly illustrates the behavior of $C(\varepsilon^*, n, m)$ as ε^* grows and ε^{*-1} passes through the values $-\mathrm{Re}(\lambda_{p,l}) \sim (|p|+2l)^{-2}$ with $p = n, m$. If $\lambda_{p,l} \in \mathbb{R}$, ε^{*-1} directly hits the pole. Therefore $C(\varepsilon^*, n, m)$ first grows from a finite value rapidly to a directional complex infinity $\infty e^{i\theta}$ for some θ, then back from $-\infty e^{i\theta}$ to a finite value after passing through it. Otherwise if $\lambda_{p,l} \notin \mathbb{R}$ and when l is large, ε^{*-1} does not pass through the pole, but comes very close to it. Hence, $C(\varepsilon^*, n, m)$ grows rapidly from a considerably small value to a complex value of very large modulus, then drops to a small value after passing through $-\mathrm{Re}(\lambda_{p,l})$. Moreover, for a fixed pair of p, l, we have

$$\frac{\beta_{p,l}}{\varepsilon^{*-1} + \lambda_{p,l}} \to -\frac{i}{2}\sqrt{R} J_p^2(R) H_p^{(1)}(R) \tag{4.63}$$

as $\varepsilon^* \to \infty$. Therefore, we can see that $C(\varepsilon^*, n, m)$ has very oscillatory behavior as ε^* grows.

4.4. The super-resolution phenomenon

Although $C(\varepsilon^*, n, m)$ is very oscillatory as ε^* grows, the aforementioned behavior and series decomposition of $C(\varepsilon^*, n, m)$ gives a clear explanation of the super-resolution phenomenon for high-contrast inclusions. It is because, what we have actually proved is that, in the shape derivative of the scattering coefficients of a circular domain, there are simple poles corresponding to the complex resonant states, and therefore peaks at the real parts of these resonances. Hence, as the material contrast ε^* increases to infinity and is such that it hits the real part of a resonance, the sensitivity in the scattering coefficients becomes very large and super-resolution for imaging occurs.

To put it more accurately, let us recall (3.26). Suppose $D = B(0, R)$, then for any δ-perturbation of D, D^δ, along the variational direction $h \in \mathcal{C}^1(\partial D)$, we have

$$W_{nm}(D^\delta, \varepsilon^*) - W_{nm}(D, \varepsilon^*) = \delta\, C(\varepsilon^*, n, m) \mathfrak{F}_\theta\left[h\right](n-m) + O(\delta^2)\,.$$

As one might recall from (2.28), $W_{nm}(D^\delta, \varepsilon^*)$ always decays exponentially as $|n|, |m|$ increase. Hence, it is always of exponential ill-posedness to recover the higher order Fourier modes of the perturbation h. The inversion process to recover the k-th Fourier mode $\mathfrak{F}_\theta\left[h\right](k)$ becomes less ill-posed if $C(\varepsilon^*, n, m)$ is large for some $n, m \in \mathbb{Z}$ such that $k = n - m$. This not only makes the respective scattering coefficients more apparent than the others, but also lowers the condition number of the inverse process to reconstruct the respective Fourier mode. From the analysis in the previous subsection, this can only be made possible when ε^{*-1} comes close to $-\mathrm{Re}(\lambda_{p,l})$ for some $p = n, m$ and for some $l \in \mathbb{N}$.

Now, suppose ε^* is close to the following resonant value $\left(\frac{K\pi}{2R} - \frac{\pi}{4R}\right)^2$ where $K \in \mathbb{N}$ is large. Then, from the fact that the eigenvalues $\lambda_{p,l}$ of the operators $\widetilde{K}_p^{(1)}$ follow the asymptotics:

$$-\lambda_{p,l}^{-1} \sim \left(\frac{\pi(|p| + 2l)}{2R} - \frac{\pi}{4R}\right)^2, \tag{4.64}$$

we see that ε^{*-1} is close to $-\mathrm{Re}(\lambda_{p,l(p)}^{-1})$ for all $p \in \mathbb{Z}$ such that $|p| + 2\,l(p) = K$ for some $l(p) \in \mathbb{N}$. Therefore, ε^{*-1} comes close to $-\mathrm{Re}(\lambda_{K,0}^{-1}), -\mathrm{Re}(\lambda_{K-2,1}^{-1}), -\mathrm{Re}(\lambda_{K-4,2}^{-1}), \ldots, -\mathrm{Re}(\lambda_{K-2[\frac{K}{2}],[\frac{K}{2}]}^{-1})$ simultaneously where $[\cdot]$ is the floor function. This in turn boosts up the magnitudes of all the terms $\frac{\beta_{p,l(p)}}{\varepsilon^{*-1} + \lambda_{p,l(p)}}$

whenever p is of the form $p = -K + 2s$, $s = 0, 2, \ldots, K$. These terms dominate the series $s_{2,p}(\varepsilon^*)$, hence we obtain the following approximations of $s_{2,p}(\varepsilon^*)$ for all $p = -K + 2s$, $s = 0, 2, \ldots, K$:

$$s_{2,p}(\varepsilon^*) \approx -\frac{i}{2}\sqrt{R} J_p^2(R) H_p^{(1)}(R) \frac{(K-0.5)^{-2}}{4^{-1}\pi^2 R^{-2} \varepsilon^{*-1} - (K-0.5)^{-2}} \,.$$

Now we see from Theorem 4.9 that the coefficients $C(\varepsilon^*, n, m)$ have the following approximations for $n, m \in \mathbb{Z}$ when ε^* is very close to the resonant values $\left(\frac{K\pi}{2R} - \frac{\pi}{4R}\right)^2$ for large K:

$$C(\varepsilon^*, n, m) \quad \begin{cases} \approx & M_{n,m,R} \, (K-0.5)^{-6} \left(4^{-1}\pi^2 R^{-2} \varepsilon^{*-1} - (K-0.5)^{-2}\right)^{-2} \\ & \quad \text{if both of } n, m \text{ have the form } -K+2s,\ s = 0, 2, \ldots, K \,; \\ \approx & M_{n,m,R} \, (K-0.5)^{-4} \left(4^{-1}\pi^2 R^{-2} \varepsilon^{*-1} - (K-0.5)^{-2}\right)^{-1} \\ & \quad \text{if only one of } n, m \text{ has the form } -K+2s,\ s = 0, 2, \ldots, K \,; \\ & \text{is very small otherwise,} \end{cases}$$

where $M_{n,m,R}$ are some constants depending only on n, m and R. Here, the term $\left(4^{-1}\pi^2 R^{-2} \varepsilon^{*-1} - (K-0.5)^{-2}\right)^{-1}$ is very large, and makes the Fourier coefficients $\mathfrak{F}_\theta[h](n-m)$ visible for $n, m \in \{-K+2s : s = 1, 2, \ldots, K\}$ for accurate classification of the shapes. The above mechanism is possible only when ε^* increases up to one of the resonant values $\left(\frac{K\pi}{2R} - \frac{\pi}{4R}\right)^2$ when K is large. This explains the increasing likelihood of obtaining super-resolution as ε^* increases.

Now, for a given ε^*, consider the following bounded linear map over the space $l^2_\pm(\mathbb{C})$ of two-sided sequences $(a_l)_{l=-\infty}^{\infty}$ such that $\sum_{l=-\infty}^{\infty} a_l^2 < \infty$,

$$\begin{aligned} A(\varepsilon^*) : l^2_\pm(\mathbb{C}) &\to l^2_\pm(\mathbb{C}) \otimes l^2_\pm(\mathbb{C}) \\ (a_l)_{l=-\infty}^{\infty} &\mapsto (C(\varepsilon^*, n, m)\, a_{n-m})_{n,m=-\infty}^{\infty} \,. \end{aligned} \tag{4.65}$$

By Theorem 3.3, we know the shape derivative of $(W_{nm}(D, \varepsilon^*))_{n,m=-\infty}^{\infty}$ in the variational direction h is given by

$$\mathcal{D}\, W(D, \varepsilon^*)[h] = A(\varepsilon^*) \mathfrak{F}_\theta[h] \,. \tag{4.66}$$

Hence, we can conclude that the least-squared map

$$\begin{aligned} [A(\varepsilon^*)]^*[A(\varepsilon^*)] : l^2_\pm(\mathbb{C}) &\to l^2_\pm(\mathbb{C}) \\ (a_l)_{l=-\infty}^{\infty} &\mapsto \left(\sum_{n-m=l} |C(\varepsilon^*, n, m)|^2 \, a_l \right)_{l=-\infty}^{\infty} \end{aligned} \tag{4.67}$$

is a diagonal operator, and the l-th singular value $s_l(A)$ is of the form

$$s_l(A) = \sqrt{\sum_{n-m=l} |C(\varepsilon^*, n, m)|^2} \,. \tag{4.68}$$

Therefore, from the above analysis on $C(\varepsilon^*, n, m)$ when ε^* is close to the resonant values $\left(\frac{K\pi}{2R} - \frac{\pi}{4R}\right)^2$, we can observe that the singular values s_l become large and comparable to each other, making the inversion of many Fourier modes well-conditioned. This implies a much higher resolution of the modes of h, and also for reconstructing the geometry of D^δ in the linearized case. This provides a good understanding towards the recently observed phenomenon of super-resolution in the physics and engineering communities.

5. Numerical experiments

In this section, we present some numerical experiments on the behaviors of the scattering coefficients for some domains as the contrast ε^* grows, and numerically illustrate the phenomenon of super-resolution.

In the following 2 examples, we consider an infinite domain of homogeneous background medium with its material coefficient being 1. An inclusion D^δ is then introduced as a perturbation of a circular domain $D = B(0, R)$ for some $R > 0$ and $\delta > 0$ lying inside the homogeneous background medium, with its contrast chosen to be $\varepsilon^* = a_{m,l}^2/R^2 - 1$ running over all m, l such that $a_{m,l} \leq 18.901$. The exact values of the zeros of Bessel functions are found in [27].

In order to generate the far-field data for the forward problem and the observed scattering coefficients, we use the SIES-master package developed by H. Wang [28].

The forward problem is solved by computing the solutions (ϕ_m, ψ_m) of (2.8) for $|m| \leq 25$ using rectangular quadrature rule with mesh-size $s/1024$ along the boundary of the target, where s denotes the length of the inclusion boundary. The scattering coefficients of D^δ of orders (n, m) for $|n|, |m| \leq 25$ are then calculated as the Fourier transform of the far-field data.

In order to test the robustness of the super-resolution phenomenon, we introduce some multiplicative random noise in the scattering coefficients in the form:

$$W_{nm}^\gamma(D^\delta, \varepsilon^*) = W_{nm}(D^\delta, \varepsilon^*)\left(1 + \gamma(\eta_1 + i\eta_2)\right), \tag{5.1}$$

where η_i, $i = 1, 2$, are uniformly distributed between $[-1, 1]$ and γ refers to the relative noise level. In both examples below, we always set the noise level to be $\gamma = 5\%$.

Since the purpose of our numerical experiments is to illustrate the phenomenon of super-resolution as ε^* increases, we assume that both R and ε^* are known and use the following regularized inversion method suggested from the linearized problem (3.26) to recover the k-th Fourier mode for $|k| \leq 50$ from the observed noisy scattering coefficients $W_{nm}^\gamma(D^\delta, \varepsilon^*)$, $|n|, |m| \leq 25$:

$$\delta\mathfrak{F}_\theta\left[h\right]^{\text{recovered}}(k) = \sum_{n-m=k,\, |n|,|m|\leq 25} \frac{W_{nm}^\gamma(D^\delta, \varepsilon^*) - W_{nm}(D, \varepsilon^*)}{C(\varepsilon^*, n, m) + \alpha}, \tag{5.2}$$

where α is a regularization parameter. The coefficients $W_{nm}(D, \varepsilon^*)$ used in the inversion process are calculated using the same method as previously mentioned for the forward problem without adding noise, and the coefficients $C(\varepsilon^*, n, m)$ are calculated by the following approximations

$$C(\varepsilon^*, n, m) \approx \left(W_{nm}(D^{\delta_0}(n-m), \varepsilon^*) - W_{nm}(D, \varepsilon^*)\right)/\delta_0 \tag{5.3}$$

for $|n|, |m| \leq 25$, where $D^{\delta_0}(k)$ are defined as domains with the following boundaries for $|k| \leq 50$,

$$\partial D^{\delta_0}(k) := \{\tilde{x} = R(1 + \delta_0 e^{ik\theta}) \,:\, \theta \in (0, 2\pi]\} \tag{5.4}$$

with δ_0 chosen to be $\delta_0 = 0.1$.

Example 1 As a toy example, we first consider a flori-form shape D^δ described by the following parametric form (with $\delta = 0.1$):

$$r = 0.3(1 + \delta\cos(3\theta) + 2\delta\cos(6\theta) + 4\delta\cos(9\theta)), \quad \theta \in (0, 2\pi], \tag{5.5}$$

which is a perturbation of the domain $D := B(0, 0.3)$; see Figure 3 (left) for the domain and Figure 3 (right) for the comparison between the domains D^δ and D.

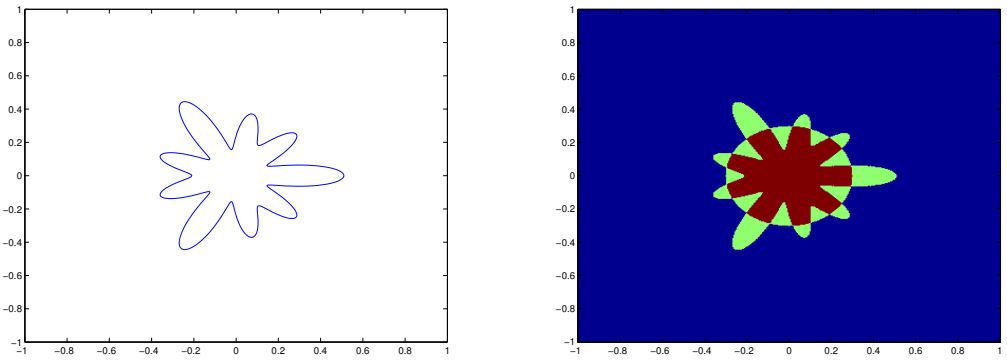

Figure 3: Inclusion shape in Example 1. Left: shape of the domain; Right: comparisoin of the domain with a circle.

The relative magnitudes of the scattering coefficients $\max_{|m-n|=k} |W_{nm}(D^\delta, \epsilon^*)| / \max_{m\neq n} |W_{nm}(D^\delta, \epsilon^*)|$ are plotted for $k = 6, 9$ in Figure 4.

From Figure 4, we can clearly observe that, as ε^* grows, the relative magnitude of the scattering coefficient corresponding to the $\pm k$-th Fourier mode grows from a smaller magnitude to larger magnitude, and the peaks become apparent when ε^* hits the respective zeros of the Bessel functions.

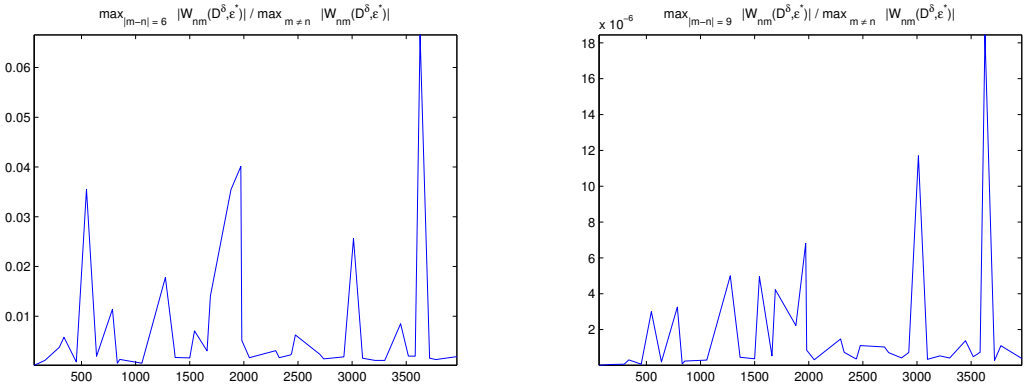

Figure 4: Relative magnitudes of the scattering coefficients in Example 1. Left: the fraction of $\max_{|m-n|=6}\{|W_{nm}(D^\delta, \epsilon^*)|\} / \max_{m\neq n}\{|W_{nm}(D^\delta, \epsilon^*)|\}$, Right: the fraction of $\max_{|m-n|=9}\{|W_{nm}(D^\delta, \epsilon^*)|\} / \max_{m\neq n}\{|W_{nm}(D^\delta, \epsilon^*)|\}$.

From the relative magnitudes shown in the above figures, we observe that the off-diagonal scattering coefficients are more apparent and are therefore best conditioned for inversion when $\varepsilon^* = 1971.2481, 3627.456$. The scattering coefficients of the respective contrasts are plotted in Figure 5 (left), together with $\varepsilon^* = 63.2669$ corresponding to the first zero of J_0 as a comparison.

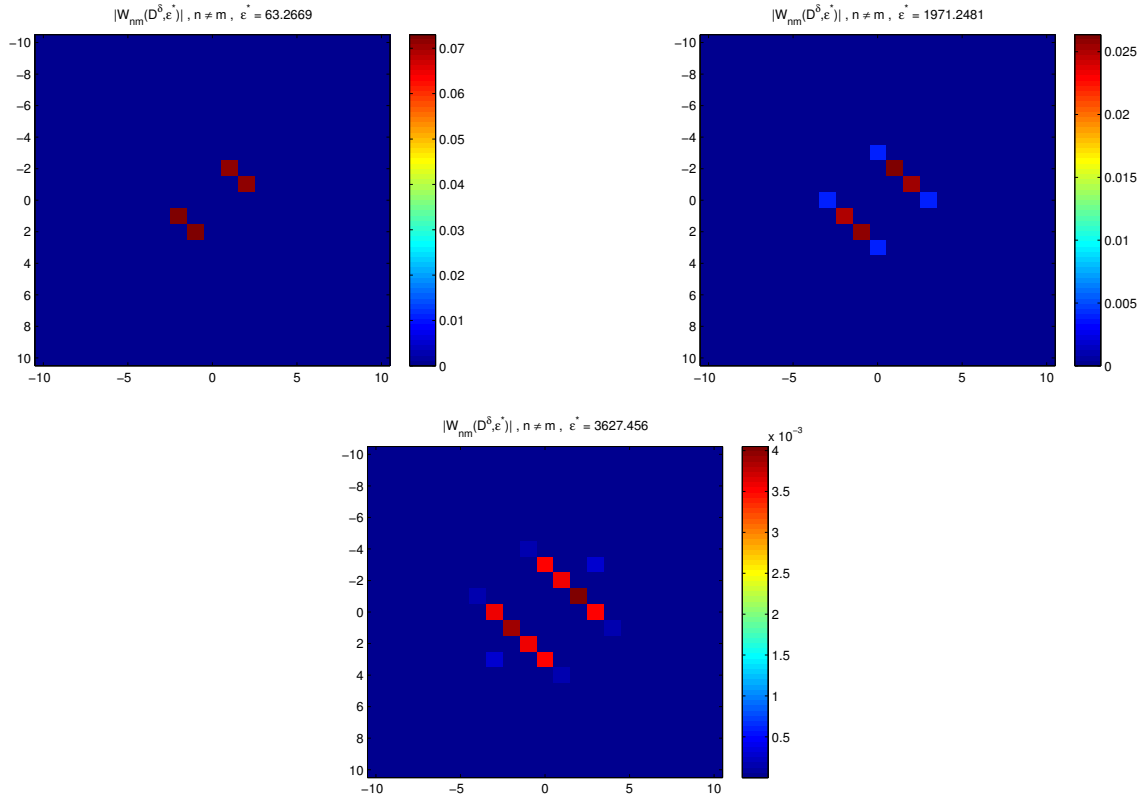

Figure 5: Illustration of super-resolution in Example 1: magnitude of scattering coefficients, $|W_{nm}(D^\delta, \epsilon^*)|$ where $-10 \leq m, n \leq 10$. Left: $\varepsilon^* = 63.2669$; right: $\varepsilon^* = 1971.2481$; bottom: $\varepsilon^* = 3627.456$

We notice from Figure 6 that the scattering coefficients corresponding to higher Fourier modes become more apparent as ε^* increases. We then apply the aforementioned inversion process, with the regularization parameter chosen as $\alpha = 1 \times 10^{-8}$. The magnitudes of the recovered Fourier modes and the reconstructed domains are shown in Figures 6 and 7, respectively. We can clearly see that the fine features are more and more apparent as ε^* grows along the specific contrasts that we choose. Notice also that the fine features are of a magnitude smaller than 0.4, which is much smaller than half of the operating wavelength, π.

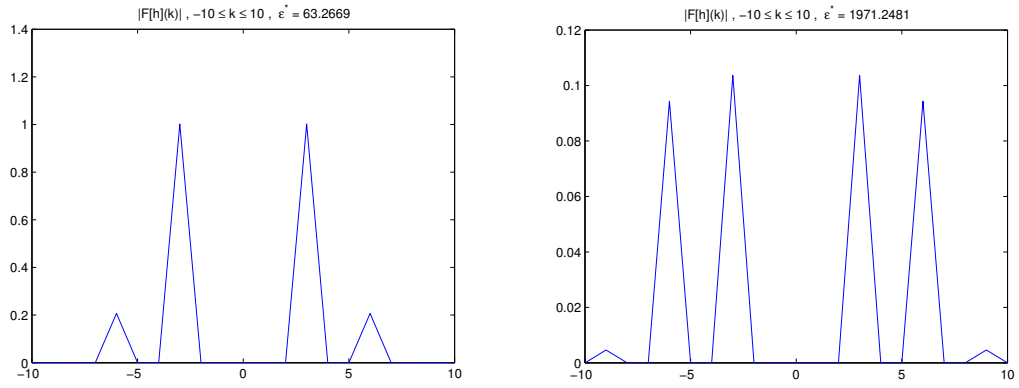

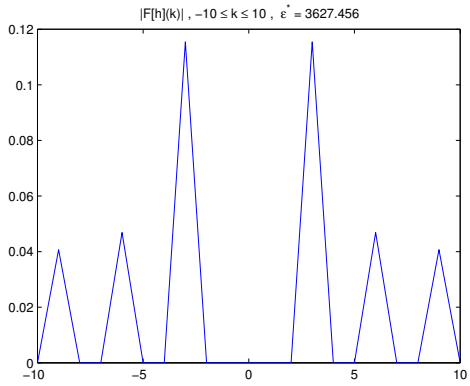

Figure 6: Illustration of super-resolution in Example 1: magnitude of recovered Fourier coefficients, $\mathfrak{F}_\theta\left[h\right]^{\text{recovered}}(k), -10 \leq k \leq 10$. Left: $\varepsilon^* = 63.2669$; right: $\varepsilon^* = 1971.2481$; bottom: $\varepsilon^* = 3627.456$.

In fact, with fine features are of a magnitude smaller than $0.4 \approx 0,1\pi$, we do not expect to recover any of these feature with incidence field of wavelength 2π. The original domain has a shape with boundary purturbation consisting of 3 Fourier modes, i.e. $k = 3, 6, 9$. As we expected from exponential ill-posedness, we do not usually expect to recover the high Fourier modes in the purturbation, especially for $k = 9$ in normal situation. However in our experiment, we can see that as the constrast increases and hits some of the values $\varepsilon^* = a_{m,l}^2/R^2 - 1$, the higher Fourier modes becomes more apparent. In particular, as seen from Figures 6 and 7, with $\varepsilon^* = 63.2669$, only the 3-th Fourier mode is present and the magnitude overshoots, at $\varepsilon^* = 1971.2481$, the 6-th Fourier mode comes out, and when $\epsilon^* = 3627.456$, even the 9-th Fourier mode becomes notable. We cannot expect the recovered magnitude of the respective Fourier modes to be exact considering the severe exponential ill-posed-ness nature, the long wave-length of the incidence as well as noise added. However, the very fact that even the 9-th Fourier modes becomes notable when it represents features of only $1/20$ of the wavelength of the incidence is very exciting, and confirms the super-resolution phenomenon observed in experiments.

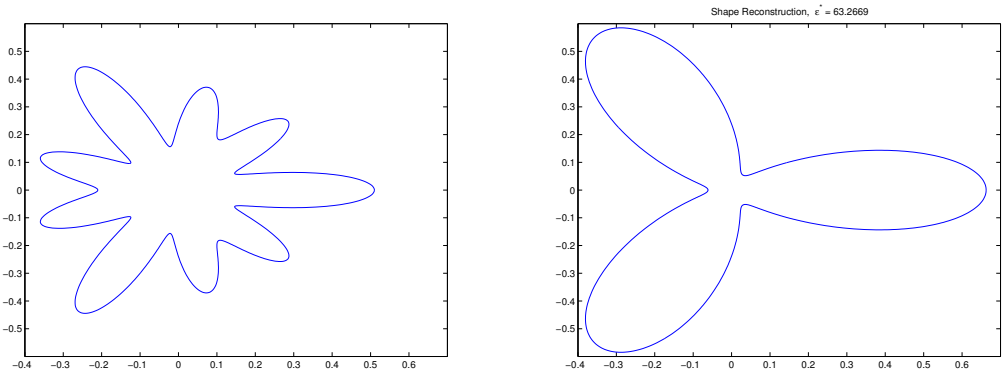

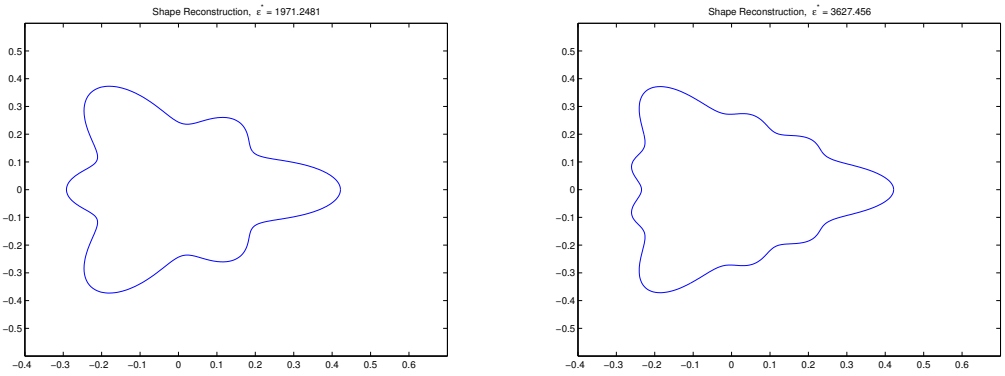

Figure 7: Illustration of super-resolution in Example 1: exact and recovered domains. Left top: exact domain. Right top: $\varepsilon^* = 63.2669$; left bottom: $\varepsilon^* = 1971.2481$; right bottom: $\varepsilon^* = 3627.456$.

Example 2 We try the following right-angled isosceles triangle D^δ, which is a perturbation of the domain $D := B(0, 0.2)$; see Figure 8 (left) for the domain and Figure 8 (right) the comparison between the domains D^δ and D. This case is substantially harder, since the perturbation h consists of many Fourier modes and is no longer smooth.

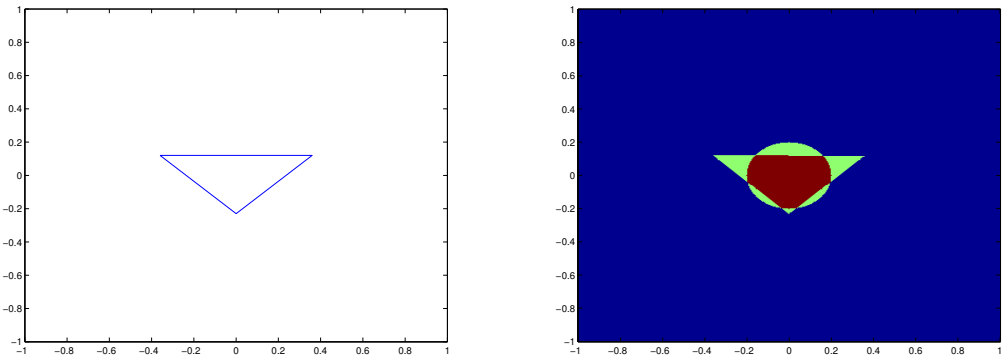

Figure 8: Inclusion shape in Example 2. Left: shape of the domain; Right: comparisoin of the domain with a circle.

The relative magnitudes of the scattering coefficients $\max_{|m-n|=k} |W_{nm}(D^\delta, \epsilon^*)| / \max_{m\neq n} |W_{nm}(D^\delta, \epsilon^*)|$ are plotted for $k = 1, 2, \ldots, 6$, in Figure 9. From this figure, we can see that the relative magnitude of the scattering coefficient corresponding to the $\pm k$-th Fourier mode comes out more often when ε^* becomes large.

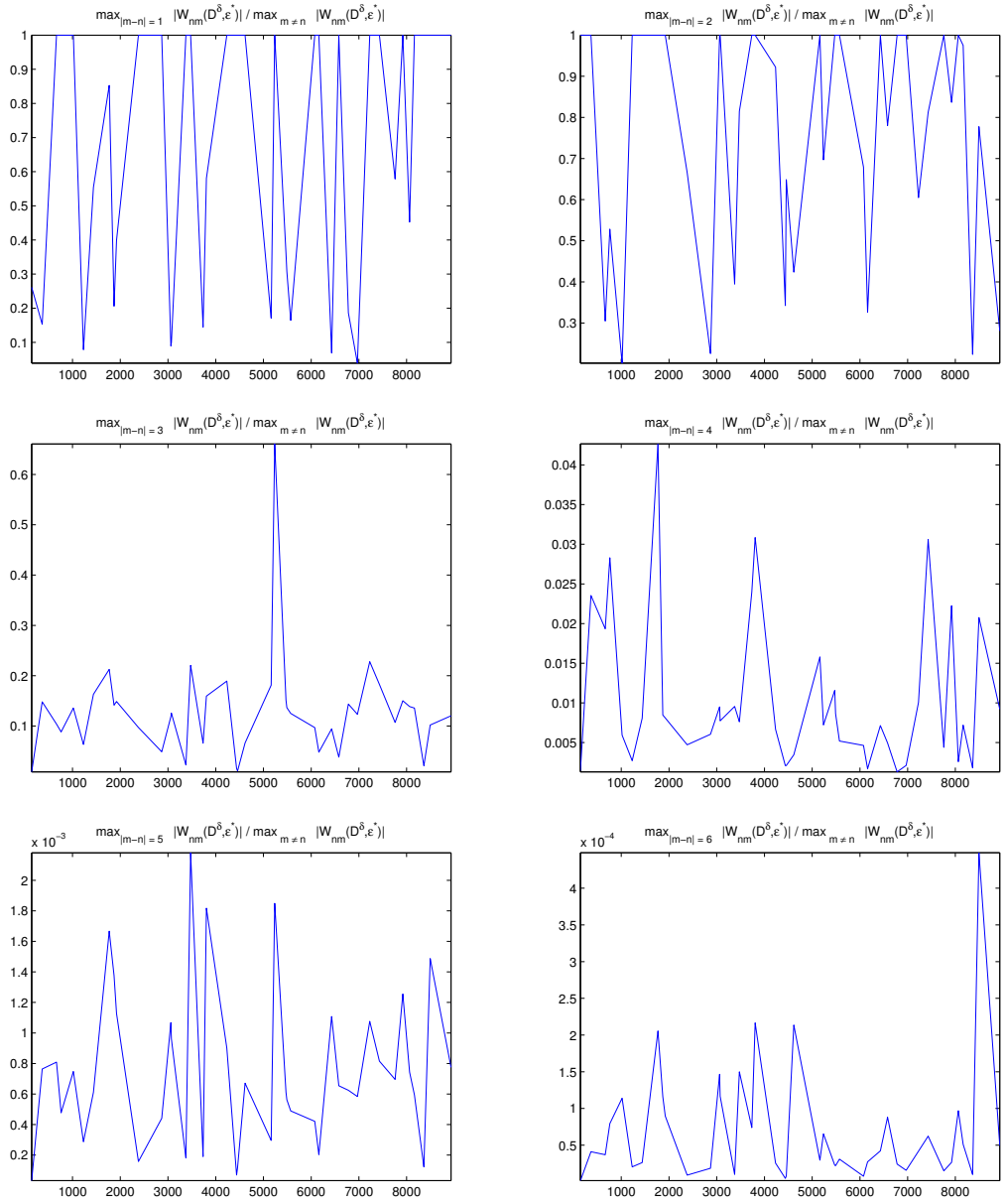

Figure 9: Relative magnitudes of the scattering coefficients in Example 2. The fraction of $\max_{|m-n|=k}\{|W_{nm}(D^\delta,\epsilon^*)|\}/\max_{m\neq n}\{|W_{nm}(D^\delta,\epsilon^*)|\}$ for $k=1,...,6$ from left to right and from top to bottom.

We observe from the relative magnitudes shown in the above figures that the scattering coefficients are best-conditioned for inversion when $\varepsilon^* = 5237.1406$. The scattering coefficients of the respective contrast are then plotted in Figure 10, together with $\varepsilon^* = 143.6006$ corresponding to the first zero of J_0 as a comparison. The aforementioned inversion process is then applied with regularization parameter chosen as $\alpha = 1 \times 10^{-6}$. Figures 11 and 12 respectively show the magnitude of the recovered Fourier modes and the reconstructed domains. We can see that the shape obtained from $\varepsilon^* = 143.6006$ provids us an understanding that the shape is with three angles, and the angle size and dimensions fit in the exact domain. However, the shape consists of three large troughs on the three edges of the triangle. The shape obtained from $\varepsilon^* = 5237.1406$ contains more high Fourier modes are present; now that the right angle is better approximated as well as less troughs present compared with that from $\varepsilon^* = 143.6006$, but

the two sharper angles becomes less apparent because the higher Fourier modes becomes more dominant.
655 Moreover, the scattering coefficients of $\varepsilon^* = 5237.1406$ are large enough for accurate classification.

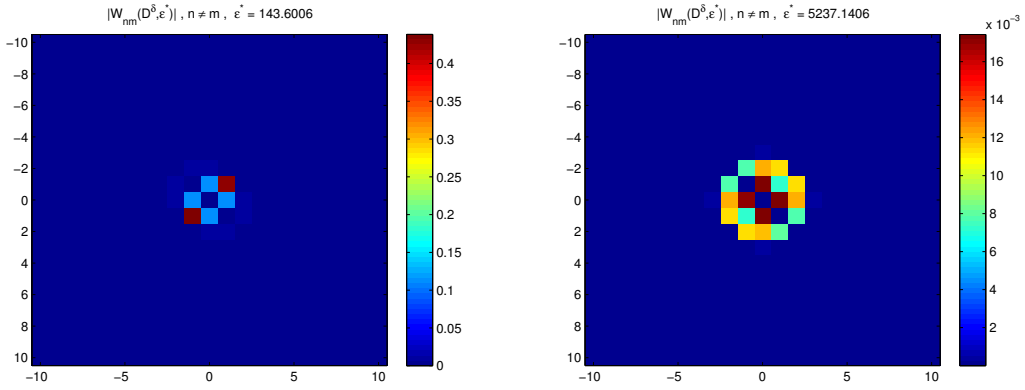

Figure 10: Illustration of super-resolution in Example 2: magnitude of scattering coefficients, $|W_{nm}(D^\delta, \epsilon^*)|$ where $-10 \leq m, n \leq 10$. Left: $\varepsilon^* = 143.6006$; right: $\varepsilon^* = 5237.1406$.

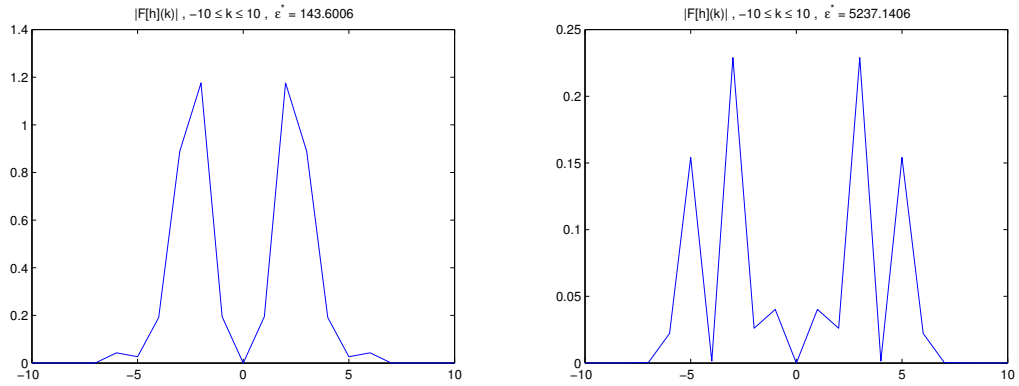

Figure 11: Illustration of super-resolution in Example 2: magnitude of recovered Fourier coefficients, $\mathfrak{F}_\theta\left[h\right]^{\text{recovered}}(k), -10 \leq k \leq 10$. Left: $\varepsilon^* = 143.6006$; right: $\varepsilon^* = 5237.1406$.

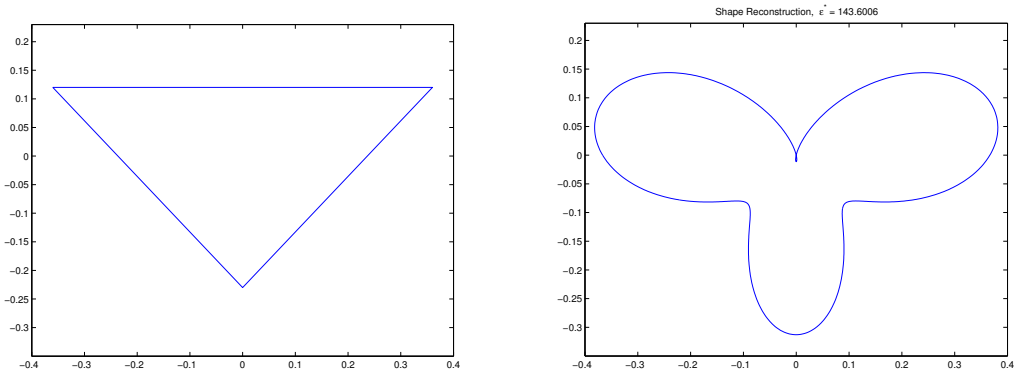

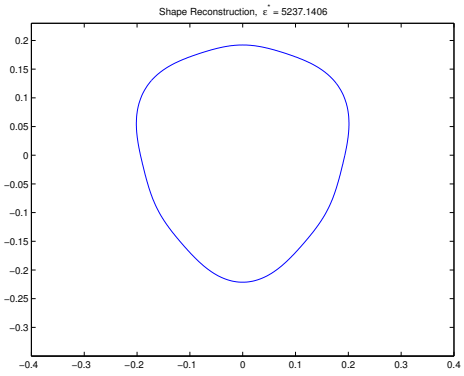

Figure 12: Illustration of super-resolution in Example 2: exact and recovered domains. Left : exact domain. Right: $\varepsilon^* = 143.6006$; bottom: $\varepsilon^* = 5237.1406$.

6. Concluding remarks

In this paper, we have for the first time established a mathematical theory about super-resolution in the context of imaging high-contrast inclusions. We have found both analytically and numerically that at some high resonant values of the contrast, super-resolution in reconstructing the shapes of the inclusions can be achieved.

Our approach opens a new avenue for mathematical imaging and focusing in resonant media. Many challenging problems are still to be solved in this direction. It would be very interesting to generalize our approach to justify the fact that super-resolution can be achieved using structured light illuminations [29, 30]. It is also a very challenging yet important problem to extend our theory to a general shape to provide an explanation of super-resolution for non-circular domains. Furthermore, it would be both mathematically and physically very interesting to develop our approach for electromagnetic and elastic wave imaging problems of high-contrast inclusions.

References

[1] H. Ammari, J. Garnier, W. Jing, H. Kang, M. Lim, K. Sølna, H. Wang, Mathematical and statistical methods for multistatic imaging, Vol. 2098, Springer, 2013.

[2] H. Ammari, H. Kang, H. Lee, M. Lim, Enhancement of near-cloaking. part ii: The helmholtz equation, Communications in Mathematical Physics 317 (2) (2013) 485–502.

[3] H. Ammari, M. P. Tran, H. Wang, Shape identification and classification in echolocation, SIAM Journal on Imaging Sciences 7 (3) (2014) 1883–1905.

[4] H. Ammari, An introduction to mathematics of emerging biomedical imaging, Vol. 62, Springer, 2008.

[5] H. Ammari, E. Bonnetier, Y. Capdeboscq, Enhanced resolution in structured media, SIAM Journal on Applied Mathematics 70 (5) (2009) 1428–1452.

[6] G. Bao, J. Lin, Near-field imaging of the surface displacement on an infinite ground plane, Inverse Probl. Imag 7 (2013) 377–396.

[7] G. Bao, P. Li, Near-field imaging of infinite rough surfaces, SIAM Journal on Applied Mathematics 73 (6) (2013) 2162–2187.

[8] H. Ammari, H. Zhang, A mathematical theory of super-resolution by using a system of sub-wavelength helmholtz resonators, Communications in Mathematical Physics 337 (1) (2015) 379–428.

[9] H. Ammari, J. Garnier, J. De Rosny, K. Sølna, Medium induced resolution enhancement for broad-band imaging, Inverse problems 30 (8) (2014) 085006.

[10] F. Lemoult, M. Fink, G. Lerosey, Acoustic resonators for far-field control of sound on a subwavelength scale, Physical Review Letters 107 (6) (2011) 064301.

[11] F. Lemoult, A. Ourir, J. de Rosny, A. Tourin, M. Fink, G. Lerosey, Time reversal in subwavelength-scaled resonant media: beating the diffraction limit, International Journal of Microwave Science and Technology 2011.

[12] F. Lemoult, G. Lerosey, J. de Rosny, M. Fink, Resonant metalenses for breaking the diffraction barrier, Physical review letters 104 (20) (2010) 203901.

[13] G. Lerosey, J. De Rosny, A. Tourin, M. Fink, Focusing beyond the diffraction limit with far-field time reversal, Science 315 (5815) (2007) 1120–1122.

[14] S. W. Hell, Far-field optical nanoscopy, science 316 (5828) (2007) 1153–1158.

[15] H. Ammari, P. Millien, M. Ruiz, H. Zhang, Mathematical analysis of plasmonic nanoparticles: the scalar case, arXiv preprint arXiv:1506.00866.

[16] S. Arhab, G. Soriano, Y. Ruan, G. Maire, A. Talneau, D. Sentenac, P. Chaumet, K. Belkebir, H. Giovannini, Nanometric resolution with far-field optical profilometry, Physical review letters 111 (5) (2013) 053902.

[17] G. Popov, G. Vodev, Resonances near the real axis for transparent obstacles, Communications in mathematical physics 207 (2) (1999) 411–438.

[18] H. Ammari, Y. T. Chow, J. Zou, The concept of heterogeneous scattering coefficients and its application in inverse medium scattering, SIAM Journal on Mathematical Analysis 46 (4) (2014) 2905–2935.

[19] J. B. Conway, A course in functional analysis, Vol. 96, Springer Science & Business Media, 2013.

[20] G. Bao, F. Triki, Error estimates for the recursive linearization of inverse medium problems, Journal of Computational Mathematics (2010) 725–744.

[21] G. N. Watson, A treatise on the theory of Bessel functions, Cambridge university press, 1995.

[22] I. Gohberg, M. G. Krein, Introduction to the theory of linear nonselfadjoint operators, Vol. 18, American Mathematical Soc., 1988.

[23] O. F. Bandtlow, Estimates for norms of resolvents and an application to the perturbation of spectra, Mathematische Nachrichten 267 (1) (2004) 3–11.

[24] M. Abramowitz, I. A. Stegun, et al., Handbook of mathematical functions (1966).

[25] T. Carleman, Zur theorie der linearen integralgleichungen, Mathematische Zeitschrift 9 (3) (1921) 196–217.

[26] H. Ammari, H. Zhang, Super-resolution in high-contrast media, in: Proc. R. Soc. A, Vol. 471, The Royal Society, 2015, p. 20140946.

[27] C. L. Beattie, Table of first 700 zeros of bessel functionsjl (x) and j'l (x), Bell System Technical Journal 37 (3) (1958) 689–697.

[28] Sies-master package, http://www.math.ens.fr/~hanwang/software/examples/Helmholtz_R2/demo.html.

[29] M. G. Gustafsson, Surpassing the lateral resolution limit by a factor of two using structured illumination microscopy, Journal of microscopy 198 (2) (2000) 82–87.

[30] M. G. Gustafsson, Nonlinear structured-illumination microscopy: wide-field fluorescence imaging with theoretically unlimited resolution, Proceedings of the National Academy of Sciences of the United States of America 102 (37) (2005) 13081–13086.